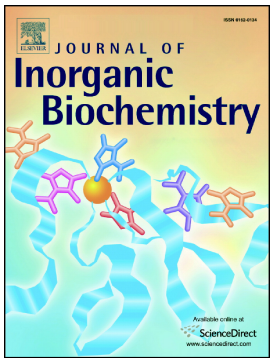

Development, evaluation and effect of anionic co-ligand on the biological activity of benzothiazole derived copper(II) complexes

Surbhi Jain, Kishalay Bhar, Shreetama Bandyopadhayaya, Vikas K. Singh, Chandi C. Mandal, Suman Tapryal, Anuj K. Sharma

PII: S0162-0134(20)30202-6

DOI: https://doi.org/10.1016/j.jinorgbio.2020.111174

Reference: JIB 111174

To appear in: *Journal of Inorganic Biochemistry*

Received date: 7 April 2020

Revised date: 28 June 2020

Accepted date: 28 June 2020

Please cite this article as: S. Jain, K. Bhar, S. Bandyopadhayaya, et al., Development, evaluation and effect of anionic co-ligand on the biological activity of benzothiazole derived copper(II) complexes, *Journal of Inorganic Biochemistry* (2020), https://doi.org/10.1016/j.jinorgbio.2020.111174

Development, Evaluation and Effect of Anionic Co-ligand on the Biological Activity of Benzothiazole Derived Copper(II) Complexes

Surbhi Jain[a], Kishalay Bhar[a], Shreetama Bandyopadhayaya[b], Vikas K. Singh[c], Chandi C. Mandal[b], Suman Tapryal[c], Anuj K. Sharma[a]*

[a]*Department of Chemistry, School of Chemical Sciences and Pharmacy, Central University of Rajasthan, Bandarsindri, District Ajmer, Rajasthan, 305817, India.*

[b]*Department of Biochemistry, School of Life Sciences, Central University of Rajasthan, Bandarsindri, District Ajmer, Rajasthan, 305817, India.*

[c]*Department of Biotechnology, School of Life Sciences, Central University of Rajasthan, Bandarsindri, District Ajmer, Rajasthan, 305817, India.*

Abstract. Research on development of novel metal based anti-cancer agents continues with its popularity among bioinorganic community. Benzothiazole, an important heterocyclic pharmacophore, was chosen as a valuable and useful scaffold for the synthesis of novel copper(II) complexes. Three new copper(II) complexes obtained from the synthesis of newly synthesized benzothiazole based *N*-(benzo[d]thiazol-2-ylmethyl)-N-methyl-2-(pyridin-2-yl)ethan-1-amine (*btzpy*) ligand with $CuCl_2$ [Cu(*btzpy*)Cl_2] (**1**), $Cu(NCS)_2$ [Cu(*btzpy*)$(NCS)_2$] (**2**), and $Cu(NO_3)_2$ [Cu(*btzpy*)$(NO_3)(H_2O)]NO_3$ (**3**) were isolated and characterized by physical and spectroscopic measurements, including single-crystal X-ray structures. The interaction of complexes **1** and **3** with calf thymus (CT)-DNA was investigated using ethidium bromide fluorescence quenching assay and weak intercalation with K_{SV} values of 9.8×10^2 M^{-1} and 8.2×10^2 M^{-1}, respectively was observed. All three complexes have shown DNA cleavage of supercoiled plasmid DNA forming single nicked and double nicked forms in the presence of external reducing agents like 3-mercaptopropionic acid (3-MPA) and ascorbic acid. The water-soluble complexes **1** and **3** also show prominent hydrolytic DNA cleavage. From the DPPH (2,2-diphenyl-1-picrylhydrazyl) radical scavenging assay, it was observed that complex **2** also exhibits good antioxidant properties. The cytotoxicity of complexes **1-3** was tested against the lung cancer cell line (A549) and complex **2** with -NCS moiety shows maximum activity in the micromolar range. A rationale for the observed activity is proposed in light of the other properties of these molecules.

1. Introduction

Cancer is the second leading cause of death in the entire world. Cancer alone caused approximately 9.6 million deaths in 2018. 1 out of 6 people around the globe dies due to cancer [1]. Out of all the types, breast and lung cancer are the most common types with 2.09 million cases reported for both in the last year. The majority of the cases (~70%) are reported in low- and middle-income countries [1]. Since the serendipitous discovery of the anticancer property of cisplatin by Rosenberg *et al*. in 1964 [2] and its success in treating malignancies, there has been a massive upsurge in the development of metal-based therapeutics. Many different metals like Ru, Fe, Pd, Au, Ti, Ga, V, Co, etc. have been developed and used as anticancer agents [3-7]. Certain complexes of Ru (such as NAMI-A (imidazolium-*trans*-tetrachloro(dimethylsulfoxide)imidazoleruthenium(III)), KP1019 (*trans*-[tetrachlorobis(1*H*-indazole)ruthenate(III)]), and NKP-1339 (sodium *trans*-[tetrachloridobis(1*H*-indazole)ruthenate(III)]) [8-10] have reached clinical trials along with Fe based tamoxifen [11] and Cu based casiopeína [12]. Several recent review articles highlight the latest developments and the journey of metal based antitumor drugs [13-15]. Copper complexes induce apoptosis in cancer cells via several mechanisms like by generating reactive oxygen species (ROS) [16, 17], proteasome inhibition [18], targeting enzymes [19], DNA damage [20, 21], etc.; thus, making it difficult for resistance development. Since the body has a very well-defined mechanism for copper homeostasis, copper becomes a very suitable candidate for therapeutic purposes [22]. Several copper complexes that act as artificial nucleases have been explored for their anticancer potential and many of them have shown exceptional activity with toxicity profiles better than the known anticancer drugs [23]. Out of all the reported complexes, Casiopeínas®, a class of mixed chelate copper(II) complex with a general formula $[Cu(N\text{-}N)(N\text{-}O)\ H_2O]NO_3$ or $[Cu(N\text{-}N)(O\text{-}O)H_2O]NO_3$ (where, N-N = diimines as 1,10- phenanthroline, 2,2-bipyridine, or their substituted analogues, N-O = aminoeidate and O-O = acetylacetonate, salicylaldehidate), are gaining lot of attention as two of the complexes from this family, Casiopeína III-ia (aqua, 4,4-dimethyl-2,2'-bipyridine, acetylacetonato copper(II) nitrate) and Casiopeína II-Gly could enter in phase I clinical trials [24, 25]. The former is being tested against acute myeloid leukemia where it has been shown that the complex induces fragmentation of DNA and oxidation of the base. This suggests that the mode of action for the complex involves generation of ROS after the metal center has been reduced [26]. Hernández-Lemus et al. demonstrated that Casiopeína II-Gly

shows its effect by enhancing the metabolism of metals and by blocking the migration and proliferation rate of cancerous HeLa cells [27]. Despite all the merits, no copper-based therapeutic has been approved so far for human use. Therefore, more efforts are required towards designing and synthesis of novel copper compounds for use as potential anticancer agents.

Over the years, it has been established that the cytotoxic activity and the nuclease ability of the synthesized metal complexes are vastly dependent on the organic ligand framework around it [23, 28-30]. In fact, the effect of donor atoms and structural features of the complex can affect the lipophilicity/hydrophilicity of the compound, the preferred oxidation state of the metal center and most importantly, the biological activity of the compounds [31]. Thus, we designed novel *N*,*N*,*N*-based ligand utilizing the benzothiazole (btz) moiety, an important heterocyclic pharmacophore. Btz and its derivatives are involved in a diverse range of pharmacological activities such as antimicrobial, herbicidal, pesticidal, antidiabetic, anti-inflammatory, anticonvulsant, and many more including antitumor [32, 33]. Several examples of benzothiazole based ligands [34-40] have been reported in the literature and have been evaluated for their DNA binding and activity against cancer cell lines. Considering the importance of Cu(II) and the pharmacological relevance of benzothiazole based drugs, Cu(II) complexes containing benzothiazole motifs within the ligand framework could be of valuable interest. In this lieu, we have synthesized and characterized three novel Cu(II) complexes with benzothiazole based ligand, N-(benzo[d]thiazol-2-ylmethyl)-N-methyl-2-(pyridin-2-yl)ethan-1-amine (*btzpy*), having benzothiazole and pyridyl moieties. The ligand coordinates with metal mainly by nitrogen atoms of pyridyl, thiazole and the alkyl nitrogen connecting the two.

Here we report the synthesis, spectroscopic characterization, single-crystal X-ray structures of three novel Cu(II) complexes with *btzpy* ligand and different anionic co-ligands [Cu(*btzpy*)$(Cl)_2$] (**1**), [Cu(*btzpy*)$(NCS)_2$] (**2**), and [Cu(*btzpy*)$(NO_3)(H_2O)]NO_3$ (**3**). Complex **1** and **3** are water-soluble with easily dissociable -Cl^- and -NO_3^- ions, whereas complex **2** with -NCS^- ligand is soluble in organic solvents like acetonitrile, dimethylformamide (DMF), dimethyl sulfoxide (DMSO)) only. A comparative biological study of the complexes with DNA binding, Bovine Serum Albumin (BSA) binding, DNA cleavage, antioxidant properties and *in vitro* cytotoxicity against the lung cancer cell line (A549) is reported.

2. Experimental

2.1. Materials and methods

All the reagents were purchased from commercial sources and used as it is without any purification. 2-aminothiophenol was purchased from Kemphasol; chloroacetyl chloride was purchased from Molychem; 2-methylaminoethylpyridine, Calf thymus DNA (CT-DNA), ethidium bromide, Bovine Serum Albumin (BSA), DPPH (1,1-diphenyl-2-picrylhydrazyl), Trolox (6-hydroxy-2,5,7,8-tetramethychroman-2-carboxylic acid) was purchased from Sigma-Aldrich; copper chloride was obtained from Ramkem; copper perchlorate was purchased from Alfa Aesar while all other reagents (potassium carbonate, potassium iodide, copper nitrate, sodium sulfate, potassium thiocyanate) were purchased from CDH. All the solvents were distilled before use. For all biological experiments, ultra-pure Milli-Q water was used. For MTT assay, 3-(4,5-dimethylthiazol-2-yl)-2,5-diphenyltetrazoliumbromide (MTT) was purchased from Himedia (MB186). All the experiments involving CT-DNA and BSA were performed in PBS buffer (pH=7.4). The concentration of CT-DNA was calculated by measuring the absorbance at 260 nm (ε =6,600 $M^{-1}cm^{-1}$) [41]. The ratio of absorbance at 260 nm and 280 nm was 1.8-1.9, indicating that the DNA was sufficiently protein-free. The solutions were stored at 4˚C and were used within 5 days. *E. coli* DH5α cells (Invitrogen) grown overnight in incubator shaker (Thermo scientific) at 37℃, 150 rpm were used for the isolation of plasmid pET28b (+) (Novagen). The cells grown overnight were harvested for the isolation of bacterial plasmid pET28b (+). MACHERY-NAGEL Nucleospin® plasmid kit was used for the isolation and purification of the plasmid pET28b (+). The isolated plasmid pET28b (+) was used for further analysis on 1% agarose gel. 1% agarose gel was prepared in a 1× TAE (Tris base, acetic acid and EDTA) buffer by adding ethidium bromide (EtBr) (1 µg/mL). The samples were mixed with 6× DNA loading dye purple (New England Biolab, UK) before loading into the respected wells.

2.2. Physical measurements

The NMR spectra for ligand were recorded on the Bruker-500 MHz spectrometer in $CDCl_3$. Molar conductivity was measured on a Systronics Conductivity Meter-304 at room temperature in 1 mM acetonitrile solution for all the complexes and in double-distilled water for complex (**1**) and (**3**). Elemental analyses (C, H, N, S analysis) were performed on a Thermo-Scientific Flash 2000 CHNS/O Elemental Analyzer and the values were within ±0.4% of the theoretical values.

Infrared spectra were recorded as KBr pellets on a Perkin Elmer FTIR Spectrometer (Spectrum Two) in the range 4000–400 cm^{-1}. The UV-visible spectra were recorded on Agilent Cary-60 UV-vis spectrophotometer at room temperature in a cuvette of path length 1 cm. Fluorescence spectra for all the studies were recorded on the Agilent Cary Eclipse spectrophotometer at room temperature in a quartz cuvette of path length 1 cm. Cyclic voltammograms for all the complexes (**1**-**3**) were recorded on Autolab PGSTAT 302N workstation (Eco-Chemie BV, Netherlands) at room temperature under dinitrogen in dry acetonitrile using a standard three-electrode cell consisting of a glassy carbon working electrode, a platinum auxiliary electrode and Ag wire as the reference electrode. EPR was recorded on a Varian, E-112 ESR Spectrometer (for complex **1**) and on a JEOL EPR Spectrometer with X & Q band (for complexes **2** and **3**) at SAIF, IITB, Mumbai in acetonitrile: propionitrile (1:3) glass at LNT (77 K). Agarose gel electrophoresis was performed horizontal electrophoresis unit (GeNei) and run by using a Power Pac (Bio-Rad) voltage controller system. The gels were visualized and imaged under UV light using the Gel documentation system (DNR MiniLumi). The MTT assay was performed in 96 well flat-bottom tissue culture plates and the absorbance was recorded at 530 nm using Spectro Star Nano Elisa Reader (BMG Labtech). Human lung cancer cells, A549 which were procured from NCCS cell repository, Pune, India were used for the cell culture-based experiments. The cells were grown in Dulbecco's Eagles Modified Medium (DMEM) (HyClone, SH30243.LS) which was supplemented with 10% fetal bovine serum (FBS) (HyClone, SV30160.03) and was maintained in a CO_2 incubator at 5% CO_2 at 37°C.

*2.3. Synthesis of ligand (btzpy) and copper complexes (**1**-**3**)*

The synthetic scheme has been outlined in Scheme 1.

2.3.1. Synthesis of the ligand

2.3.1.a. Synthesis of precursor 2-chloromethylbenzothiazole: The precursor for ligand synthesis was synthesized using the literature method [42]. The crude product obtained from this method was purified by column chromatography using a mixture of ethyl acetate and petroleum ether (1:9) to produce 2-chloromethylbenzothiazole as a colorless oily liquid at room temperature with 80% yield (1.2 g). Upon cooling, colorless needle-shaped crystals were obtained. ^{1}H NMR (500 MHz, $CDCl_3$) δ (ppm) = 7.96 (d, 1H); 7.77 (d, 1H); 7.32 (t, 1H); 7.13 (t, 1H); 4.04 (d, 2H).

2.3.1.b. Synthesis of btzpy ligand: The ligand was synthesized by suspending K_2CO_3 (1 g, 0.722 mmol) in acetonitrile and 2-(2-methyl aminoethyl)pyridine (98.4 mg, 0.722 mmol) was added to it. After 10 mins, 2-chloromethylbenzothiazole (133 mg, 0.722 mmol) and a catalytic amount of KI (0.1 equivalents) were added to the reaction mixture. The reaction was refluxed at 90 °C overnight. The reaction mixture was filtered to remove the excess of K_2CO_3 and acetonitrile was evaporated. Water (50 mL) was added to the reaction mixture and then the product was extracted in dichloromethane (25 × 3 mL). The combined organic phases were washed with brine (20 mL) and dried over Na_2SO_4. Evaporation of the organic phase yielded pure ligand as a brown viscous liquid in 86% yield (170 mg). ^{1}H NMR (500 MHz, $CDCl_3$) δ (ppm) = 8.49 (d, 1H, -H_l); 7.93 (d, 1H, -H_k); 7.81 (d, 1H, -H_j); 7.55 (m, 1H, -H_i); 7.39 (m, 1H, -H_h); 7.32 (m, 1H, -H_g); 7.16 (d, 1H, -H_f); 7.08 (t, 1H, -H_e); 3.99 (s, 2H, -H_d); 3.03 (d, 2H, -H_c); 2.98 (d, 2H, -H_b); 2.45 (s, 3H, -H_a). ^{13}C NMR (125 MHz, $CDCl_3$) δ (ppm) = 173.30 (-C_o), 160.04 (-C_p), 153.29 (-C_n), 149.27 (-C_l), 136.28 (-C_i), 135.47 (-C_m), 125.71 (-C_h), 124.72 (-C_g), 123.33 (-C_f), 122.72 (-C_k), 121.69 (-C_j), 121.23 (-C_e), 59.80 (-C_d), 57.66 (-C_b), 42.71 (-C_a), 36.42 (-C_c).

*2.3.2. Synthesis of [Cu(btzpy)Cl_2] (**1**)*

$CuCl_2{\cdot}2H_2O$ (103 mg, 0.6 mmol) in methanol (10 mL) was added to a stirred solution of ligand (*btzpy*) (170 mg, 0.6 mmol) in dichloromethane (10 mL). After stirring the reaction at room temperature for 24 hours, the blue colored precipitate obtained was filtered, dried and washed with diethyl ether. The product was recrystallized in acetonitrile by slow evaporation. Dark blue coloured crystals suitable for Single Crystal XRD were obtained. Yield: 165 mg (66 %). Elemental analysis for $C_{16}H_{17}Cl_2CuN_3S$: Calcd. C, 45.99; H, 4.10; N, 10.06; S, 7.67%; found: C, 45.97; H, 4.06; N, 10.10; S, 7.89%. FTIR (KBr disc, cm^{-1}): 3736 (m) (υ_{C-H}), 1697 (m) ($\upsilon_{C=N}$, $\upsilon_{C=C}$), 1513 (s), 752 (s), 710 (m). UV-Vis (λ_{max}/nm, (ε, $M^{-1}cm^{-1}$)) in acetonitrile: 221 (2.4×10^4), 235 (2.3×10^4), 260 (1.5×10^4), >800. UV-Vis (λ_{max}/nm, (ε, $M^{-1}cm^{-1}$))in H_2O: 237 (1.5×10^4), 256 (1.4×10^4), 656 (1.1×10^2). Molar conductance, Λ_M =10 Ω^{-1} cm^2 mol^{-1} (1 mM solution in acetonitrile at 25˚C); Λ_M =300 $\Omega^{-1}cm^2$ mol^{-1} (1 mM solution in H_2O at 25˚C) (expected range for 1:2 electrolyte in H_2O: 145–273 $\Omega^{-1}cm^2$ mol^{-1} [43]).

*2.3.3. Synthesis of [Cu(btzpy)(NCS)$_2$] (**2**)*

$Cu(NCS)_2$ was generated in situ by mixing $Cu(ClO_4)_2 \cdot 6H_2O$ (260 mg, 0.70 mmol) and K(NCS) (137 mg, 1.40 mmol) in a 1:2 ratio in methanol. The $K(ClO_4)$ generated was filtered while the pale-yellow colored solution of $Cu(NCS)_2$ was added to a solution of ligand (*btzpy*) (200 mg, 0.70 mmol) in dichloromethane (10 mL). The reaction was stirred at room temperature for 24 hours. The green-colored precipitate obtained was filtered, dried and washed with diethyl ether. The product was recrystallized in acetonitrile by slow evaporation. Green colored crystals suitable for Single Crystal XRD were obtained. Yield: 143 mg (44%). Elemental analysis for $C_{18}H_{17}CuN_5S_3$: Calcd. C, 46.68; H, 3.70; N, 15.12; S. 20.77%; found: C, 46.49; H, 3.57; N, 15.07; S, 20.81%. FTIR (KBr disc, cm^{-1}): 3736 (m) (υ_{C-H}), 2080 (m) (υ_{CN} (NCS)), 2040 (s) (υ_{CN} (NCS)), 1513 (s), 772 (s) (υ_{CS} (NCS)). UV-Vis (λ_{max}/nm, (ε, $M^{-1}cm^{-1}$)) in acetonitrile: 235 (2.2×10^4), 255 (1.4×10^4), 405 (9.3×10^2), 713 (1.7×10^2). Molar conductance, Λ_M =50 Ω^{-1} cm^2 mol^{-1} (1 mM solution in acetonitrile at 25˚C).

*2.3.4. Synthesis of [Cu(btzpy)(NO_3)(H_2O)](NO_3) (**3**)*

$Cu(NO_3)_2$ (131 mg, 0.70 mmol) in methanol (10 mL) was added to a stirred solution of ligand (*btzpy*) (200 mg, 0.70 mmol) in dichloromethane (10 mL). The reaction was stirred at room temperature for 24 hours. The blue colored precipitate obtained was filtered, dried and washed with diethyl ether. The product was recrystallized in acetonitrile by slow evaporation. Dark blue colored crystals suitable for Single Crystal XRD were obtained. Yield: 157 mg (46 %). Elemental analysis for $C_{16}H_{19}CuN_5O_7S$: Calcd. C, 39.40; H, 3.82; N, 14.32; S, 6.56%; found: C, 39.77; H, 3.50; N, 14.72; S, 6.96%. FTIR (KBr disc, cm^{-1}): 3736 (m) (υ_{C-H}), 1412 (s) ($\upsilon_{C=C}$), 1380 (s), 1280 (vs), 1016 (m), 761 (s). UV-Vis (λ_{max}/nm, (ε, $M^{-1}cm^{-1}$)) in acetonitrile: 233 (1.7×10^4), 258 (1.3×10^4), 290 (5.4×10^3), 630 (1.5×10^2). UV-Vis (λ_{max}/nm, (ε, $M^{-1}cm^{-1}$)) in H_2O: 236 (2.3×10^4), 256 (1.9×10^4), 658 (1.8×10^2). Molar conductance, Λ_M =110 Ω^{-1} cm^2 mol^{-1} (1 mM solution in acetonitrile at 25˚C); Λ_M =250 $\Omega^{-1}cm^2$ mol^{-1} (1 mM solution in H_2O at 25˚C) (expected range for 1:2 electrolyte in H_2O: 145–273 $\Omega^{-1}cm^2$ mol^{-1} [43]).

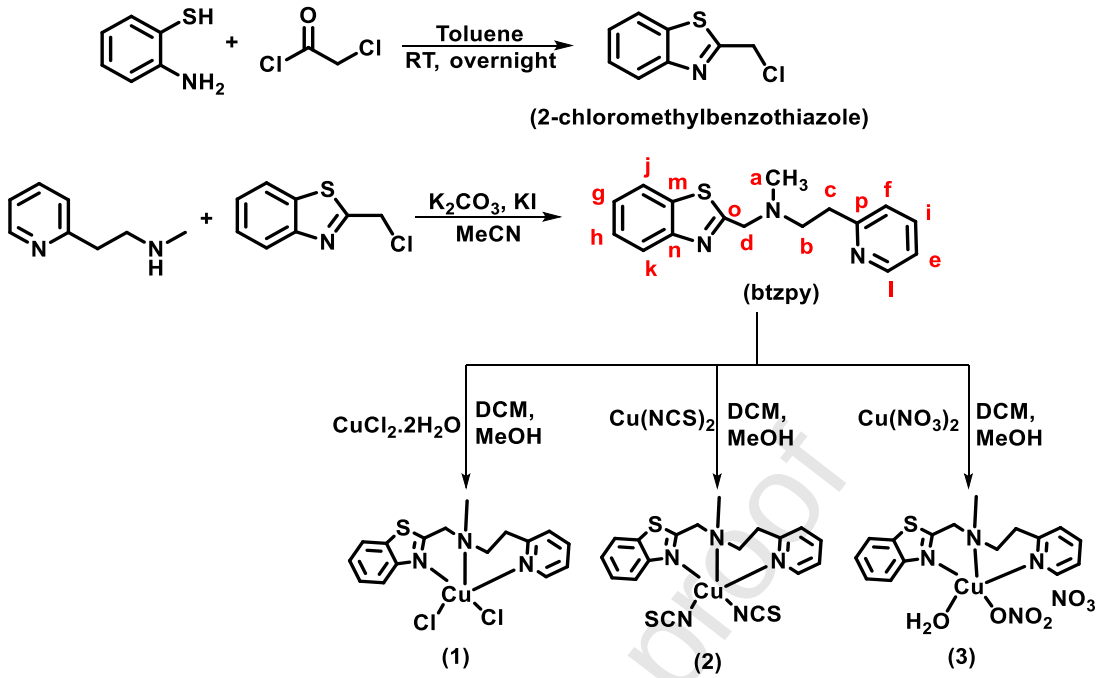

Scheme 1. Synthetic scheme for ligand (*btzpy*) and copper complexes (**1-3**).

2.4.Single crystal X-ray crystallographic data collection and refinement

Suitable single crystals of **1-3** for X-ray analysis were obtained by slow evaporation of a concentrated solution of acetonitrile. Crystallographic data were collected at 296 K on Bruker APEX-II CCD Diffractometer using graphite monochromated Mo-K_α radiation (λ = 0.71073 Å) at USIC, The University of Burdwan, Burdwan. The structures were solved by direct methods and refined by full-matrix least-squares methods based on F^2 using SHELXT[44] and SHELXL[45] programs. The non-hydrogen atoms were subjected to refinement by anisotropic displacement parameters. Hydrogen atoms were given isotropic *U* values 1.2 times that of the atom to which they are bonded and placed in calculated positions when possible. PLATON[46] and OLEX2[47] programs were used for preparing materials for publication. CCDC reference numbers for **1-3** are 1994356, 1994357 and 1994358, respectively.

2.5. Stability determination

The stability of all the copper complexes was assessed at room temperature by recording UV-visible spectra at different time intervals from 0 to 24 hours on the Agilent Cary-60

spectrophotometer. Solutions of complexes **1** and **3** were prepared in H_2O while for complex **2**, acetonitrile was the solvent of choice due to its limited solubility in H_2O.

2.6. DNA binding studies

The ethidium bromide (EtBr)-DNA adduct is highly fluorescent due to the intercalation of EtBr in between DNA base pairs. This fluorescence can be quenched upon the interaction of another molecule with DNA. The EtBr displacement assay could be performed for complex **1** and **3**, only as complex **2** was soluble in organic solvents like acetonitrile and DMSO and precipitated out when added into the buffer solution. Stock solutions of DNA, EtBr, and complexes **1** and **3** were prepared in PBS buffer of pH 7.6. Increasing concentrations of complex (0- ~100 μM) were titrated into the EtBr-DNA solution where the final concentration of CT-DNA, as well as EtBr, was 18 μM. The emission of all the solutions was recorded from 490 nm to 800 nm when excited at 480 nm. The excitation and emission slit widths were kept constant throughout the experiment at 10 nm., each. The data were analyzed using the Stern-Volmer quenching plot:

$$I_0/I = 1 + K_{SV}[Q];$$

where I_o is the fluorescence intensity of the EtBr-DNA solution, I is the fluorescence intensity of the solution after the addition of complex, [Q] is the concentration of the complex in the cuvette and K_{SV} is the Stern-Volmer quenching constant.

2.7. DNA nuclease activity

The DNA cleavage ability of the synthesized complexes was determined by Agarose gel electrophoresis. Supercoiled plasmid DNA (pET-28b) was incubated with the complex and reducing agent (3-mercaptopropionic acid (3-MPA) or Ascorbic Acid) for 1 h at 37ºC in 10 μL reaction volume. Complex **1** and **3** were dissolved in H_2O while the stock solution of complex **2** was made in acetonitrile where the final volume of acetonitrile in the Eppendorf was ~10%. The ratio of complex concentration to reductant concentration was 2:5 in all the reactions. The Agarose gel electrophoresis experiment was run in 0.8% agarose gel prepared in 1× TAE buffer, at a constant voltage of 4-5 V/cm. Ethidium bromide of concentration 1 μg/mL was added while preparing the gel. Before loading the samples in respected wells, they were mixed with 6× DNA loading dye purple (New England Biolab, UK).

2.8. Protein interaction studies

The protein (BSA) binding of the complexes was evaluated using the steady-state fluorescence quenching experiments which were performed on Agilent Cary Eclipse fluorescence spectrometer at room temperature. 10 μM solution of BSA, prepared in PBS buffer of pH 7.6, was used for the study. The emission spectra were recorded from 285-510 nm (λ_{em} (max.) = 350 nm) where the tryptophan residue of BSA was excited at 280 nm. Synchronous fluorescence emission titrations at a wavelength difference of $\Delta\lambda$ = 60 nm and $\Delta\lambda$ = 15 nm were performed using the same concentration of BSA with varying concentrations of the complexes. Similar to the DNA binding studies, the protein interaction studies could also be carried out for complex **1** and **3**, only. The binding constant was calculated using the Stern Volmer Equation.

2.9.Antioxidant Assay

To analyze the antioxidant properties of the synthesized complexes, DPPH (1,1-diphenyl-2-picrylhydrazyl) radical scavenging assay was performed. DPPH is a stable radical at room temperature and the solution is deep violet in color. When DPPH accepts an electron from another molecule, it becomes diamagnetic and pale yellow in color. As a result, the absorption of the solution at 517 nm is significantly quenched. To study the antioxidant activity of the complexes, a 100 μM stock solution of DPPH in methanol was used. In a 96-well plate, 66 μL of DPPH with different concentrations of the complexes were used and the final volume was made up to 100 μL using methanol. The solutions were incubated for 20 mins in the dark after which the absorption at 517 nm was recorded on a UV-visible spectrophotometer (ThermoFisher, MultiScan Go). For control, 66 μL of DPPH diluted with 34 μL of methanol alone was used. Trolox was used as an antioxidant standard in assay protocol. The scavenging activity (%) was calculated using the following equation:

$$Scavenging\ activity\ (\%) = \frac{A_C - A_S}{A_C} \times 100\ \%$$

where, A_C is the absorbance of only DPPH solution, and A_S is the absorbance of DPPH in presence of complexes.

2.10. Cell viability assay

The synthesized copper complexes were assessed for cytotoxicity on the A549 (human lung cancer) cell line by performing MTT cell viability assay. Approximately 5000 A549 cells/well were seeded in a 96-well tissue culture plate. The lung cancer cells were grown in DMEM supplemented with 10% FBS at 37ºC in 5% CO_2. After 24 h of seeding, the copper complexes were added in increasing concentrations over a range of 0.5 μM-50 μM. Ligand *btzpy* was also tested for activity at higher concentrations (50 μM-250 μM). An equal volume of solvent was added to the control wells. Since complex **2** was insoluble in aqueous media, the stock solution of 1 mM was prepared in DMSO. The solution was then diluted to 200 μM by adding milli-Q water. The maximum concentration of DMSO in the well plate did not exceed 5%. Control wells with DMSO up to 20% were also set where no prominent cell death was observed. The well plates were incubated for 48 h after the addition of the complexes. Later, MTT solution (5 mg/mL) was added to each well and the plate was further incubated for an hour in the incubator. Afterward, the culture media was replaced with DMSO to dissolve the formed formazan crystals. The absorbance of each well was measured at 530 nm [48, 49]. The plot of normalized percentage viability of the cells versus log concentration was plotted and fitted using non-linear regression of dose response-inhibition equation in graph pad prism for the calculation of IC_{50} values. The experiments were set up in triplicates and the values have been represented as mean ± standard deviation.

3. Results and discussion

3.1. Synthesis, stability, and characterization

The ligand (*btzpy*) was synthesized by a substitution reaction between 2-chlorobenzothiazole and 2-(2-methyl aminoethyl)pyridine (Scheme 1). The formation of the ligand was monitored by ^{1}H NMR spectroscopy. Two doublets (at 7.93; 7.81 ppm) and two triplets of benzothiazole (at 7.39, 7.32 ppm); and three -CH_2 moieties present in the ligand were characteristic peaks. The -CH_2 peak of 2-chloromethylbenzothiazole at 4.04 ppm shifted to 3.99 ppm upon ligation with the amine. In addition, the DEPT NMR spectrum also showed the presence of three -CH_2 groups in the structure (ESI Figure S1-S3). The UV-visible spectrum of the ligand shows sharp $\pi \rightarrow \pi^*$ and $n \rightarrow \pi^*$ transitions at 221 nm and 255 nm, respectively (ESI Figure S4).

The complexes (**1-3**) were synthesized by the reaction of *btzpy* ligand with $CuCl_2 \cdot 2H_2O$ (**1**), $Cu(NCS)_2$ (**2**) and $Cu(NO_3)_2$ (**3**) in dichloromethane and methanol mixture, respectively. $Cu(NCS)_2$ was synthesized *in situ* by the reaction of $Cu(ClO_4)_2 \cdot 6H_2O$ with two equivalents of potassium thiocyanate (KNCS). Complex **1** and **3** were obtained as blue colored solids while complex **2** was obtained as green colored solid. The complexes are highly colored and stable in air. Complexes **1-3** are soluble in organic solvents such as acetonitrile and DMSO. Complexes **1** and **3** are additionally soluble in H_2O, making them more feasible for biological studies. The limited solubility of complex **2** in organic solvents along with precipitation upon addition of buffer restricted the DNA and BSA binding analysis of the complex.

The elemental analyses of all three complexes show good correspondence within the accepted range of ±0.4 (ESI Figure S5-S7). The medium intensity band in FTIR at around 710 cm^{-1} in complex **1** can be assigned to the C-S stretching vibration [50]. The sharp intensity bands in the range of 1412-1513 cm^{-1} in all three complexes are assigned to the C=N stretching vibration of the benzothiazole moiety. In complex **2**, the sharp intensity bands at 2040-2080 cm^{-1} and 772 cm^{-1} are for a terminal N bound NCS for-CN and -CS stretch, respectively [51]. The presence of two types of $-NO_3$ groups in complex **3** can be observed from the two groups of IR frequencies (1380, 1016 cm^{-1} and 1280, 761 cm^{-1}). Also, a broad peak >3500 cm^{-1} shows the presence of a H_2O molecule in the system (ESI Figure S8-S10). The UV-vis spectra of the three complexes in acetonitrile have been shown in Figure 1. The complexes show strong ligand-based $\pi \rightarrow \pi^*$ and $n \rightarrow \pi^*$ transitions from 200-300 nm. The weaker and broader bands at wavelengths > 600 nm are due to the d-d transition of Cu(II) [52, 53]. In addition, complex **2** showed a sharp band at 405 nm probably due to LMCT from -NCS to Cu(II) center. Further, the stability of the complexes was assessed in suitable solvents (H_2O and acetonitrile for complex **1** and **3**, and only acetonitrile for complex **2**) by UV-vis spectroscopy. On careful analysis of the UV-vis spectra in correlation with the conductivity measurements, it was observed that in complexes **1** and **3** the anionic co-ligands dissociate when dissolved in H_2O. The *btzpy* ligand remains intact in the structure as the ligand bands (at wavelengths < 300 nm) can still be observed in the spectrum. Since only slight variations in the intensities with no prominent spectral changes in the particular solvent were observed even after 24-48 h, it indicated that the complexes are stable with no evident hydrolysis of the *btzpy* ligand in the solvents used at room temperature (ESI, Figure S11-S15).

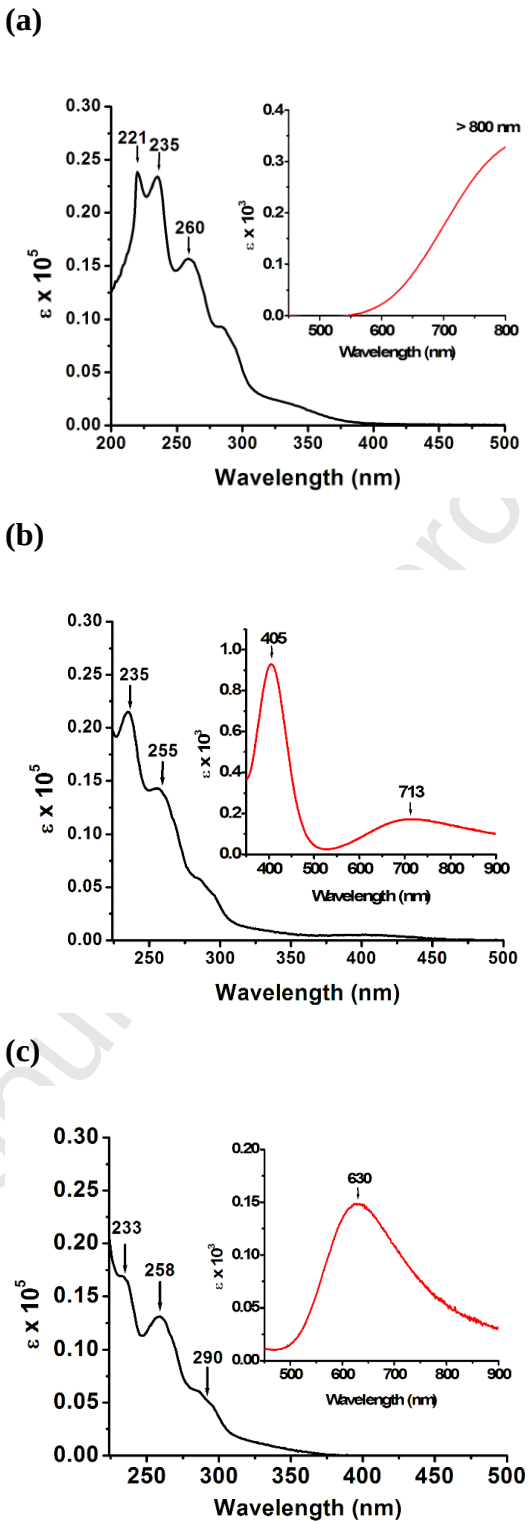

Figure 1(a-c). UV-vis spectra of copper complexes (**1-3**) recorded at 10^{-5} M; (Inset) 10^{-3} M in Acetonitrile at room temperature.

The EPR spectra for all the complexes were recorded in Acetonitrile at liquid N_2 temperature. Complex **1** shows an intermediate, rhombic EPR spectrum with g_x (2.22) > g_y (2.16) > g_z (1.99) (Figure 2). The spectrum with three g values is indicative of a penta-coordinated system with geometry in between square pyramid and trigonal bipyramid geometries [54]. The R parameter can be indicative of the predominant geometry, thereby showing the predominance of the d_z2 or d_x2- d_y2 orbital in the ground state. Here,

$$R = \frac{g_y - g_z}{g_x - g_y}$$

The value of R for complex **1** is calculated to be 2.81, i.e. greater than 1, thereby indicating that the geometry is closer to trigonal bipyramid. The crystal structure of complex **1** shows that it has a τ value of 0.72 which confirms the same geometry. Complexes **2** and **3** show normal axial EPR spectra with $g_{\|} > g_{\perp}$ (ESI, Figure S16-S17). Complexes **2** and **3** have the $g_{\|}$ value around 2.25, while the $g_{\perp}$ values are 2.08 and 2.06, respectively. These g values signify that the geometry around Cu^{2+} is square pyramidal where the ground state is the d_x2-$_y2$ orbital [55]. The EPR spectrum of complex **3** is further split into a four-line spectrum due to unpaired electron present in the d_{x2-y2} orbital. In the spectrum, three lines are well-resolved and one overlaps with the $g_{\perp}$ signal.

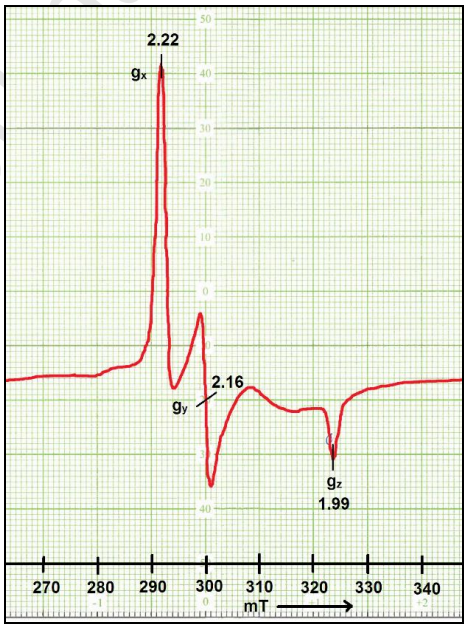

Figure 2. X-band EPR spectrum of complex **1** in acetonitrile: propionitrile (1:3) glass at LNT (77 K) (frequency 9.1 GHz and 100 kHz field) (For better viewing, the red line has been highlighted).

Further, to analyze the $Cu^{2+}/^{+}$ redox potential, the cyclic voltammograms for all three complexes were recorded. All the complexes show a quasi-reversible one-electron reduction for $Cu^{2+}/^{+}$ redox couple which indicates that the ligand can accommodate a Cu^{+} oxidation state as well (Figure 3). The anodic peak potentials (E_{pa}) for the $Cu^{2+}/^{+}$ couple for complexes **1-3** was observed at ~ 0.05 V to 0.11 V with ΔE_p ranging from 110 mV to 180 mV. The $E_{1/2}$ values for complexes **1-3** were calculated to be 0.10 V, 0.16 V, and 0.2 V, respectively. The ease of reduction of the complexes is an important aspect for the activation of the complex towards DNA cleavage as discussed in section **3.4**. Under similar conditions, the ligand (*btzpy*) showed no redox activity.

(a)

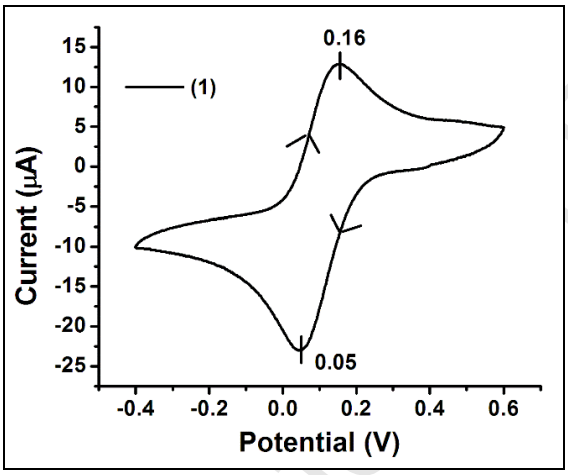

(b)

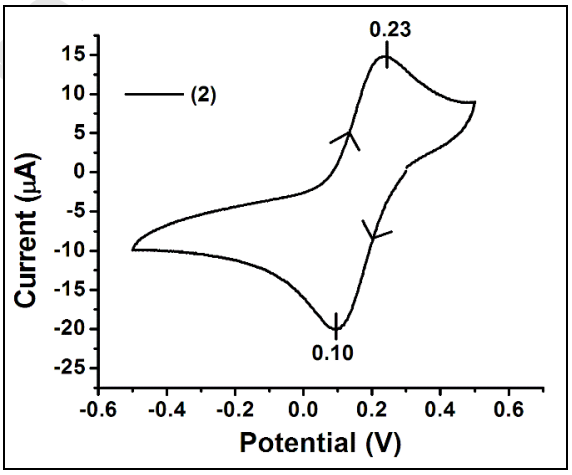

(c)

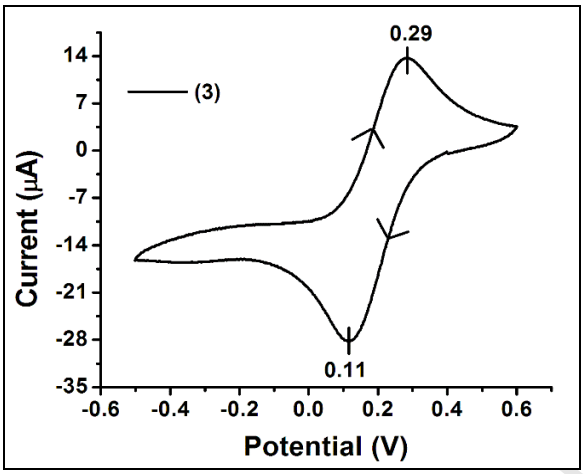

Figure 3(a-c). Cyclic voltammograms of copper complexes **1-3** at 100 mV.s^{-1} scan rate in dry Acetonitrile and 0.1 M TBAP as supporting electrolyte *vs.* Ag wire.

3.2. X-ray crystallographic studies

The geometry of three new copper(II) compounds (**1-3**) and binding mode of ligand (*btzpy*) were established by single crystal X-ray crystallography and are shown in Figure 4. Compounds **1** and **2** crystalize in triclinic system with $P\bar{1}$ space group whereas compound **3** crystallizes in monoclinic system with $P2_1/n$ space group. The crystallographic data and refinement parameters are summarized in Table S1. The selected bond distances and angles are given in Table S2.

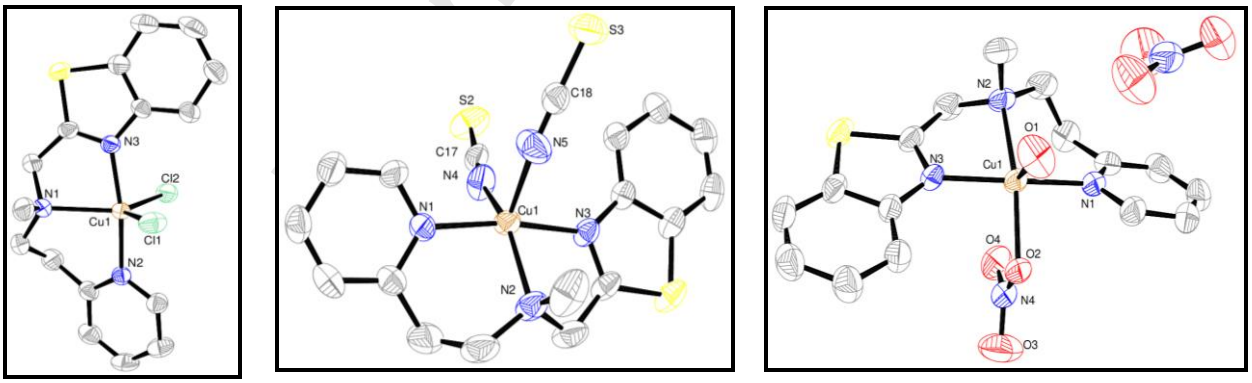

(a) **(b)** **(c)**

Figure 4. ORTEP diagrams of **1-3 (a-c)** with 50% thermal ellipsoid probability for all non-hydrogen atoms. The hydrogen atoms were omitted for clarity.

The asymmetric unit of **1** and **2** contain $[Cu(btzpy)(Cl)_2]$ and $[Cu(btzpy)(NCS)_2]$, respectively and that of **3** consists of a cationic moiety $[Cu(btzpy)(H_2O)(NO_3)]^+$ with a nitrate counter anion. In **1-3**, the *btzpy* ligand acts as a tridentate N-donor chelator and coordinates to Cu(II) ion

through pyridine N (N^{py}), amine N (N^{am}) and benzothiazole N (N^{btz}) atoms with formation of a six-membered and a five-membered chelate rings. The remaining two sites are occupied by two Cl^- ions in **1**, two NCS^- moieties in **2**, and one H_2O molecule and one NO_3^- ion in **3**. The geometry around each penta-coordinated Cu(II) ion in **1-3** is predicted by trigonality index parameter [$\tau = (\beta-\alpha)/60$; β and α are the two largest angles around Cu(II)] [56]. The values of τ are 0.72 for **1**, 0.37 for **2** and 0.10 for **3** (τ = 0 for square pyramid and τ = 1 for trigonal bipyramid) indicating distorted trigonal bipyramidal (TBP) geometry for **1** and distorted square pyramidal (SP) geometry for **3** around Cu(II) centre. However, Cu(II) centre in **2** adopts SP geometry with severe distortion towards TBP geometry. The N^{am} atom (N1) of btzpy along with the two Cl atoms form the equatorial plane while the N^{py} (N2) and N^{btz} (N3) of btzpy occupy the apical positions around TBP Cu(II) centre in **1**. The values of Cu-N and Cu-Cl bond distances are similar to that of reported compounds [57]. Further, an axial compression along Cu1-N2 and Cu1-N3 bonds (Table S2) is noticed in **1** which is consistent with a d_{z^2} electronic ground state for TBP geometry [58]. In **2** and **3**, the basal plane is formed by three N atoms (N1, N2, N3) of btzpy along with the N atom (N4) of NCS^- in **2** and the O atom (O2) of NO_3^- in **3**; while the apical site is occupied by N atom (N5) of remaining NCS^- moiety in **2** and the O atom (O1) of water molecule in **3**. The apical Cu-N/Cu-O bond distance in **2** and **3** is larger than basal Cu-N/Cu-O distances which is consistent with the SP geometry (Table S2). A comparative account of geometry related to some relevant penta-coordinated copper(II) compounds bound by bi-/tridentate chelators containing benzothiazole moiety and compounds **1-3** is summarized in Table S3.

3.3. DNA binding studies

In order to understand the interaction of complexes **1** and **3** with CT-DNA, fluorescence titrations with ethidium bromide (EtBr) bound DNA were employed. EtBr is a well-known DNA intercalator and is highly fluorescent when intercalated between DNA base pairs [59, 60]. In the free state, the fluorescence of EtBr is quenched by the solvent. EtBr bound to DNA exhibits a sharp fluorescence at around 600 nm which can be quenched upon the addition of a molecule that interacts or intercalates with DNA. Copper complexes **1** and **3** were titrated against the EtBr-DNA solution and a moderate quenching was observed along with a noticeable red-shift of ~3 nm (Figure 5). The studies indicate that although the complexes interact with DNA, they do not

intercalate within the DNA strands well. The Stern-Volmer quenching constants for complex **1** and **3** were calculated to be 9.8×10^2 M^{-1} and 8.2×10^2 M^{-1}, respectively (Figure 6). The absence of planar ligand frames and extended conjugation rings (like phenanthroline, bipyridine, etc.) is probably responsible for the similar, and weak intercalation of both the complexes.

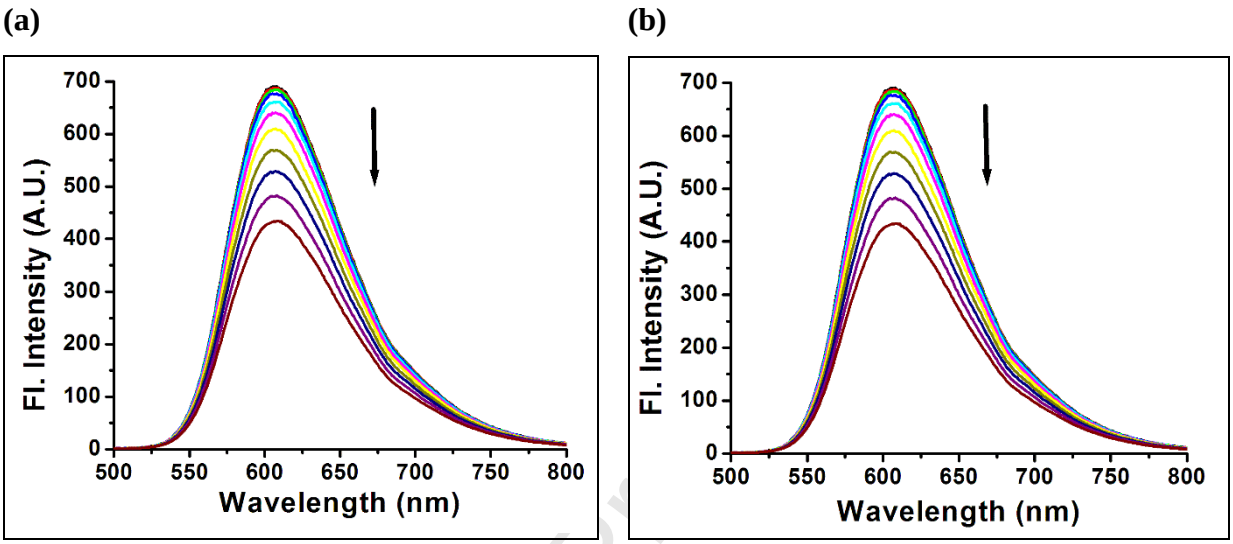

Figure 5. Plot of fluorescence emission intensity *vs.* wavelength for DNA-EtBr at different concentrations of **(a) (1)**; **(b) (3)**. The arrow shows the change in intensity of emission on increasing amount of the complex from 0 to 200 μM.

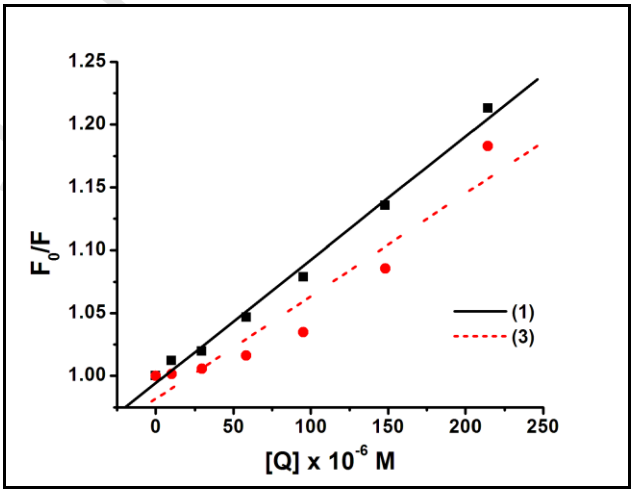

Figure 6. Stern-Volmer quenching plot of DNA-EtBr for complex **1** and **3**.

3.4. DNA nuclease activity

An artificial nuclease transforms the DNA sequentially from supercoiled to single nicked and then double nicked or linear form. Each form has a different overall structure and therefore, moves at different rates in gel electrophoresis. The supercoiled band travels the farthest and appears at the bottom while the single nicked form runs the shortest distance and appears at the top. The double nicked or linear DNA appears in between these two.

The DNA cleavage activity of all three complexes **(1-3)** was studied with pET-28b plasmid in presence of a fixed concentration of the complex with three equivalents of two different reducing agents i.e. 3-MPA and ascorbic acid (AscA). The solution of complex **2** was prepared in Acetonitrile where the final volume of Acetonitrile in the reaction vessel was around 10%. In the control plasmid, two conformations of DNA were present as evident by the two bands (Figure 7), where the upper band corresponds to single nicked form while the lower band corresponds to supercoiled form. Control experiments with 3-MPA, AscA, and ligand (*btzpy*) alone were also performed. Although 3-MPA showed no enhanced DNA cleavage, AscA and ligand alone showed a slight increment in the nicked form (Lane 3-4, Figure 7). Figure 7 shows the results of the DNA cleavage by all three complexes in the presence of 3-MPA as well as AscA. All three complexes were able to convert the supercoiled DNA form to single nicked or linear forms. It is noteworthy that all the complexes also show hydrolytic DNA cleavage, i.e. in the absence of any external reducing agent. For comparison purpose, the reactivity difference in the hydrolytic DNA cleavage for this set of compounds can be arranged as **1 > 3 > 2**, with **1** showing 100% cleavage of supercoiled form, while for the same concentration of complexes **2** and **3**, 16% and 7% of the supercoiled form is left uncleaved. The ability of these complexes to cleave DNA not only in the presence of reducing agents but also hydrolytically makes them potent nucleases. The aqueous solubility of complexes **1** and **3** may seem to play a role in the reactivity. It is possible that the dissociation of -Cl and -NO_3 anions from the molecular structure of **1** and **3**, respectively provide easy accessibility for the complex to interact with DNA, thus having a positive influence on the cleavage ability.

In hydrolytic cleavage, the phosphodiester bonds are cleaved to generate smaller fragments of DNA in the presence of water. Under ambient conditions and in absence of any catalyst, the half-life of a phosphodiester bond in DNA is ten to a hundred billion years in neutral water. This implies that in the absence of a catalyst, the DNA will not degrade for a very long time. In

general, for hydrolytic cleavage, the metal complexes act as Lewis acids which can either activate the phosphate group towards nucleophilic attack, increase the leaving group ability of the alcohol, or activate water or hydroxide to act as a nucleophile. The most accepted mechanism involves a nucleophilic attack by hydroxide or water at the phosphate backbone of DNA to form a five-coordinate intermediate which is stabilized by the catalyst (metal ion in this case). This is usually followed by cleavage of 3'-PO bond or the 5'-PO bond resulting in the scission of the DNA strand (Scheme 2) [61].

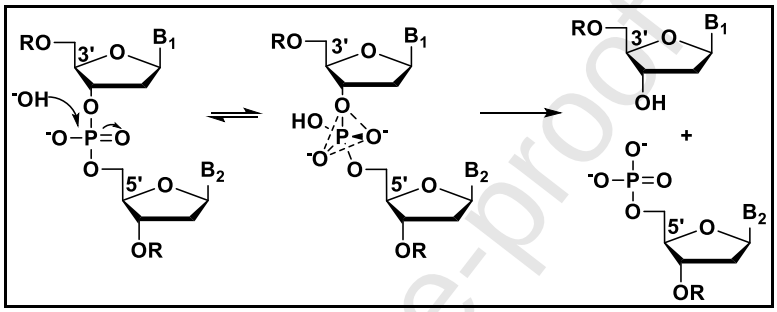

Scheme 2. The proposed reaction mechanism for the hydrolysis of DNA [61].

On the other hand, 3-MPA, or AscA can cause oxidative DNA cleavage. Unlike hydrolytic cleavage, the DNA fragments of oxidative cleavage cannot be re-ligated. All the four nucleobases [62] or the deoxyribose sugar [63] can be damaged by oxidative cleavage. The redox-active metal complexes generate the reactive intermediate species in this type of cleavage [64-66]. The cleavage occurs in three steps: Abstraction of hydrogen, addition and electron transfer. Scheme 3 depicts the process of oxidative cleavage after the abstraction of one hydrogen of deoxyribose from the C-3' terminal. Guanine is the preferred site for oxidation at the nucleic base level due to its lower oxidation potential. The hydroxyl radical reacts by adding to the heterocyclic bases of DNA. In purines, the hydroxyl radical adds to C-4, C-5, or C-8 bond while in pyramidines, it adds to C-5 or C-6 double bond [67].

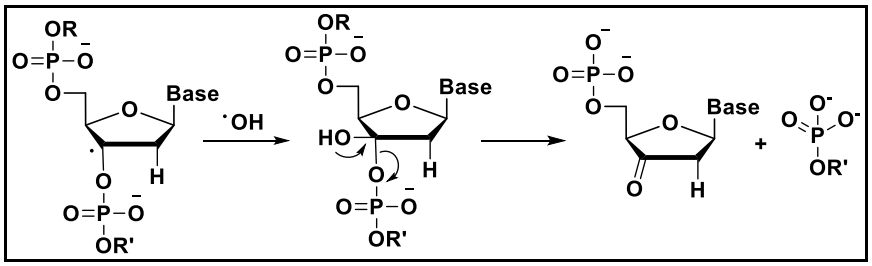

Scheme 3. Oxidative cleavage at nucleobases [61].

The most common mechanism for oxidative cleavage involves Fenton-type chemistry [68]. Mechanistic schemes with the external reducing agents (3-MPA and AscA) have been shown below [69]. Both 3-MPA and AscA, denoted as RH_x, can reduce Cu^{2+} to Cu^{+} which can react with molecular oxygen leading to the production of superoxide ion radical and regeneration of Cu^{2+}. The radical can further combine with H^{+} to form H_2O_2 which can lead to a cascade of reactions, thereby producing different ROS. The ROS thus generated can eventually cause the desired DNA cleavage activity [70].

$$Cu^{2+} + RH_x \rightarrow Cu^{+} + R^{\cdot} + xH^{+}$$

$$Cu^{+} + O_2 \rightleftharpoons Cu^{2+} + O_2^{-\cdot}$$

$$O_2^{-\cdot} + 2H^{+} \rightarrow H_2O_2$$

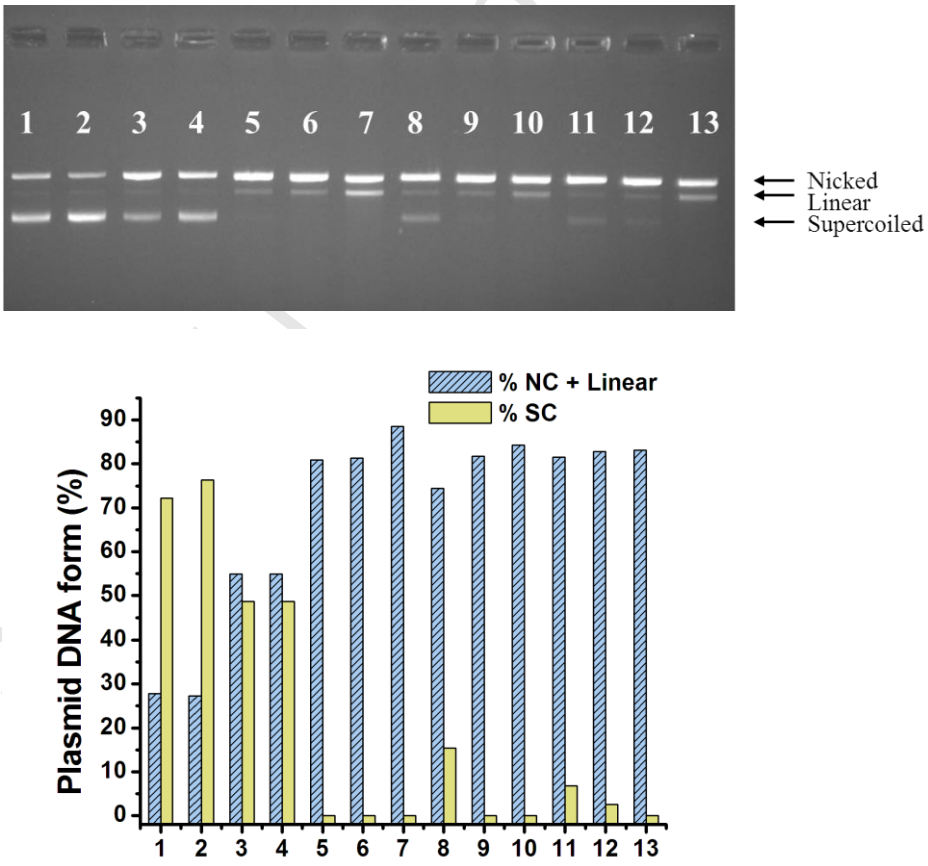

Figure 7. Analysis of DNA cleavage by complexes **1-3** using gel electrophoresis and the relative % amounts of different forms of DNA after 1 h of incubation at 37ºC. Lane 1: DNA control; Lane 2: **3-MPA** (500 μM) control; Lane 3: **AscA** (500 μM) control; Lane 4: **L (*btzpy*)** (100 μM) control; Lane 5: **1** (100 μM) control; Lane 6: **1** (100 μM) + 3-MPA (300 μM); Lane 7: **1** (100

μM) + AscA (300 μM); Lane 8: **2** (100 μM) control; Lane 9: **2** (100 μM) + 3-MPA (300 μM); Lane 10: **2** (100 μM) + AscA (300 μM); Lane 11: **3** (100 μM) control; Lane 12: **3** (100 μM) + 3-MPA (300 μM); Lane 13: **3** (100 μM) + AscA (300 μM).

3.5. Protein interaction studies

The high similarity of BSA protein with HSA protein makes it a suitable candidate to analyze the binding of the synthesized copper complexes with serum albumins. To study the interaction of the complexes with the biomolecule, the fluorescence of the tryptophan, tyrosine and phenylalanine residues present in the protein has been utilized [71, 72]. The emission of the protein can be quenched upon the interaction of the complexes due to several reasons such as the substrate binding with the protein, conformational changes occurring in the protein as a result of an interaction, subunit association, or denaturation of the protein [71, 73].

BSA solution was titrated with increasing concentrations of the copper(II) complexes and the fluorescence spectra were recorded from 290-500 nm. The maximum intensity was centered around 350 nm which decreased sequentially with negligible shift (Figure 8). The binding parameter was calculated according to the Stern-Volmer equation (Figure 9). Both the complexes show moderate binding to BSA with K_{SV} values of 1.26×10^4 M^{-1} for **1** and 1.15×10^4 M^{-1} for **3**. The structural similarity of both the complexes might be a probable reason for the similar binding constants.

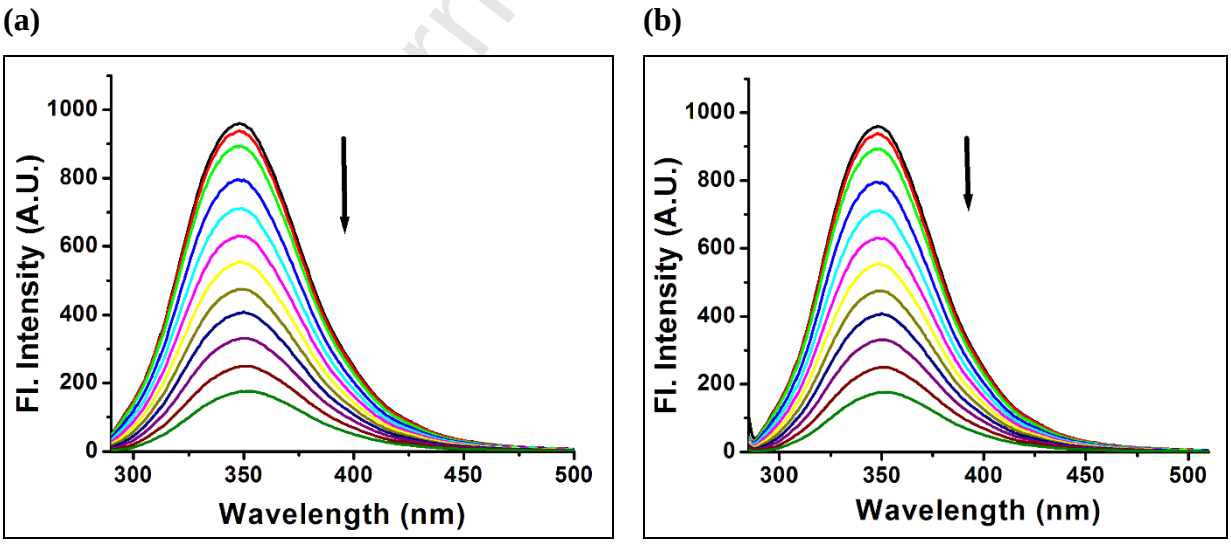

Figure 8. Plot of fluorescence emission intensity *vs.* wavelength for BSA at different concentrations of **(a) (1)**; **(b) (3)**. The arrow shows the change in intensity of emission on increasing amount of the complex from 0 to 150 μM.

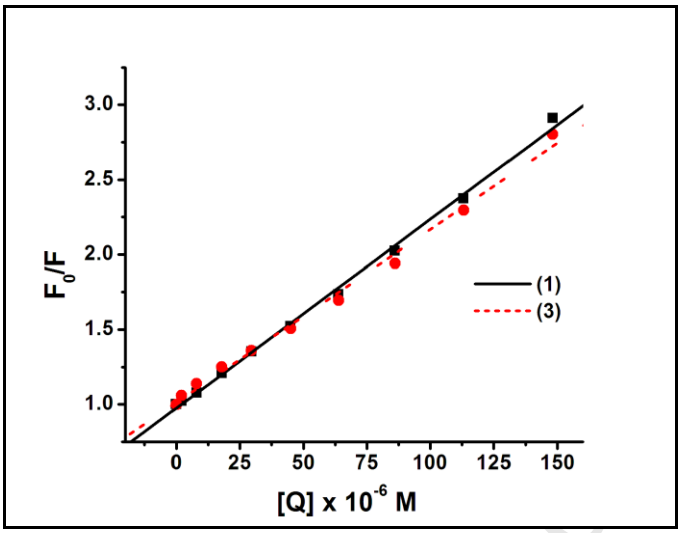

Figure 9. Stern-Volmer quenching plot of BSA for complex **1** and **3**.

3.5.1. Involvement of tryptophan and tyrosine residues in the binding

To analyze the conformational changes and the changes in the microenvironment of the BSA protein, synchronous emission spectra were recorded at $\Delta\lambda$ = 60 nm and $\Delta\lambda$ = 15 nm with increasing concentrations of complex **1** and **3** [74]. When the $\Delta\lambda$ = 60 nm, i.e. comparatively large, the spectra is mainly due to the tryptophan residue while when the $\Delta\lambda$ = 15 nm, i.e. comparatively small, then the tyrosine residue of the protein is the major contributor to the spectra. The BSA protein has three combination parts for the drugs to bind, out of which one is located at the sub-domain IIA which contains both tryptophan and tyrosine residue, whereas two are located at the IIIA sub-domain which contains only the tyrosine residue [75]. As shown in Figure 10 and 11, the fluorescence spectra for both tryptophan and tyrosine residues were quenched significantly upon the addition of the copper complexes. The interaction of the complexes with BSA was able to bring out changes in the microenvironment of the tryptophan and tyrosine residues either by decreasing the hydrophobicity, increasing the polarity, or loosening or stretching the polypeptide chains in the structure of BSA [76]. Since a clear involvement of both the residues can be seen in the process, we can say that the binding site is preferentially the sub-domain IIA of the protein.

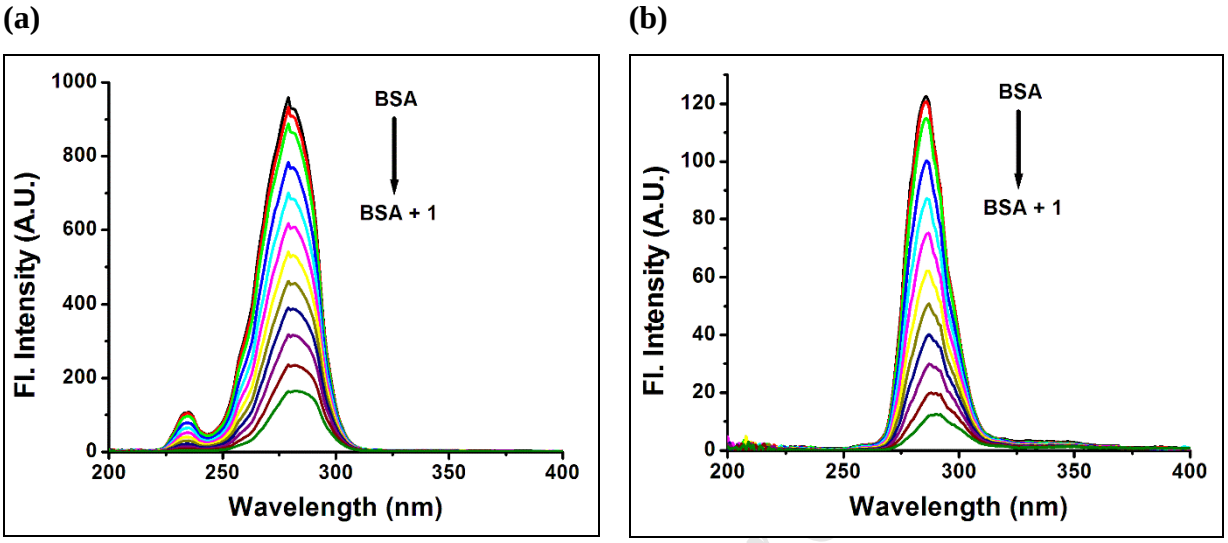

Figure 10. Synchronous fluorescence spectra of BSA with increasing concentrations of **1** at the wavelength difference of **(a)** $\Delta\lambda$ = 60 nm, **(b)** $\Delta\lambda$ = 15 nm.

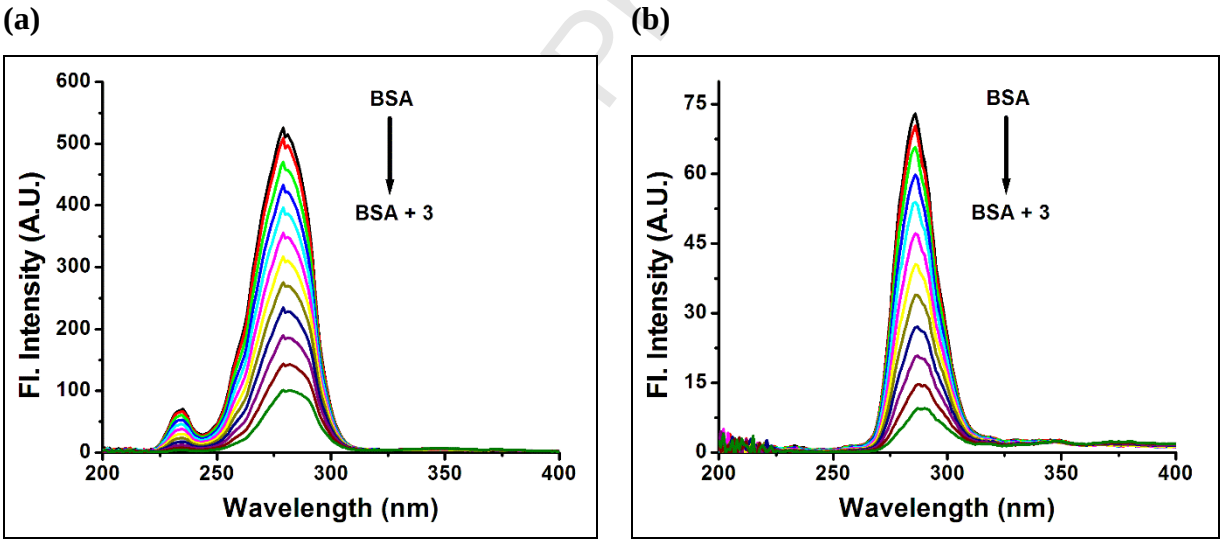

Figure 11. Synchronous fluorescence spectra of BSA with increasing concentrations of **3** at the wavelength difference of **(a)** $\Delta\lambda$ = 60 nm, **(b)** $\Delta\lambda$ = 15 nm.

3.6. Antioxidant studies

The radical scavenging activity of all three complexes was studied using DPPH. This is a simple and rapid test for antioxidant screening. Out of all the complexes tested, complex **2** shows major free radical scavenging followed by complex **3** (Figure 12). Complex **2** (200 μM) shows about

64% of scavenging of the DPPH radical while the same concentration of complex **3** shows about 23% scavenging. Complex **1** has negligible activity at this concentration. Possibly, the Cu(II) center in the complexes gets reduced to Cu(I) while transferring one electron to DPPH, thereby reducing it to diamagnetic species. Positive control of *Trolox* was also added which showed 100% scavenging activity. The antioxidant activity has a positive correlation with anticancer activity. Excessive production of free radicals in the human body can have a great impact on the etiology of various diseases [77-79] and therefore, compounds with antioxidant properties, i.e. with the ability to scavenge free radicals, may be highly beneficial and relevant for therapeutic purposes [80].

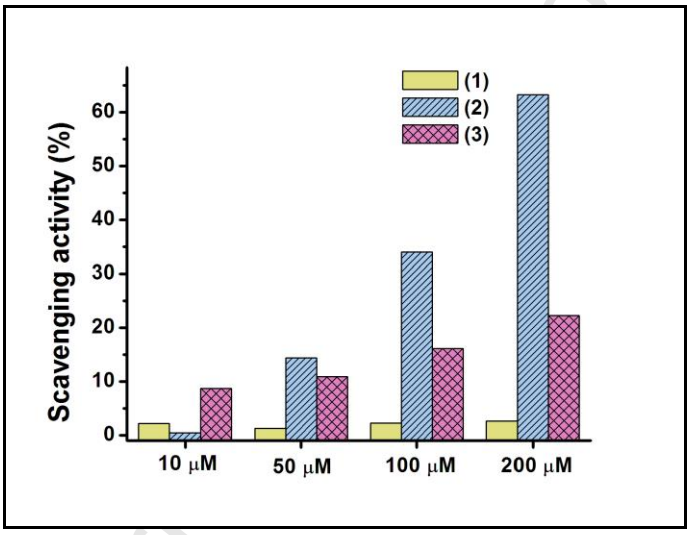

Figure 12. Free radical scavenging studies with increasing concentration of complexes **1-3**.

3.7. Cell viability assay

To compare the cytotoxic activity of all three copper complexes against human lung cancer cell line, A549, MTT assay was performed. The cytotoxicity was evaluated after 48 h of exposure of the compounds to the cells. As can be seen from Figure 13, complex **2** is most active towards the A549 cells among the three complexes. It shows the ability to suppress the proliferation of the cells in a concentration-dependent manner. The IC_{50} value of complex **2** was calculated to be 5.45 ± 0.71 μM. The complexes **1** and **3** exhibit IC_{50} values of 50.8 ± 1.18 and 51.52 ± 1.17 μM, respectively against the particular cell line used. The IC_{50} values of *btzpy* ligand was calculated to be 91.07 ± 3.28 μM (ESI, Figure S18). The higher values of IC_{50} for the ligand as compared to complexes suggest a clear involvement of the metal center for the desired activity.

It is worth to mention here that the mechanism for copper(II) complexes-mediated cytotoxicity may be triggered by their ability to bind and cleave DNA leading to cell cycle arrest and apoptosis or the generation of reactive oxygen species (ROS) which also cause cell death. Although highly detailed studies of mechanism of copper(II) complexes are scarce, few recent examples have shown that copper(II) complexes can penetrate through cell membrane and act via several different mechanistic pathways. Studies show that copper complexes have the ability to enter and accumulate in cell membrane or mitochondrial membrane; some even accumulate in the cell nuclei [81-85]. Structures of few selected complexes that support the observation of a direct correlation of individual parameters like DNA binding, metal uptake to the observed anti-proliferative activities have been given in ESI, Table S4.

Complex **2** has limited aqueous solubility and its conductivity data suggest that -NCS moiety does not dissociate from Cu(II) as compared to the other two complexes **1** & **3**. DNA cleavage studies also suggest that interaction of molecule **2** with DNA and its capability to cleave it. Since, the extent of DNA cleavage was higher by **1** & **3** as compared to **2**; it is evident that either more than one mechanism in action as far as the cell death is concerned or higher concentration of **2** is entering into the cell due to its intact form in aqueous media. The higher potential of complex **2** may be related to the presence of tightly bound -NCS groups which probably provide the required hydrophobicity to enter the cells. Several Cu(II)-NCS complexes with various ligands have been known to show different biological activities. Considering the structures of the complexes and their cell toxicity results, it can be related that the -NCS moiety linked to Cu(II) has a crucial role to play towards the anticancer activity of the complex.

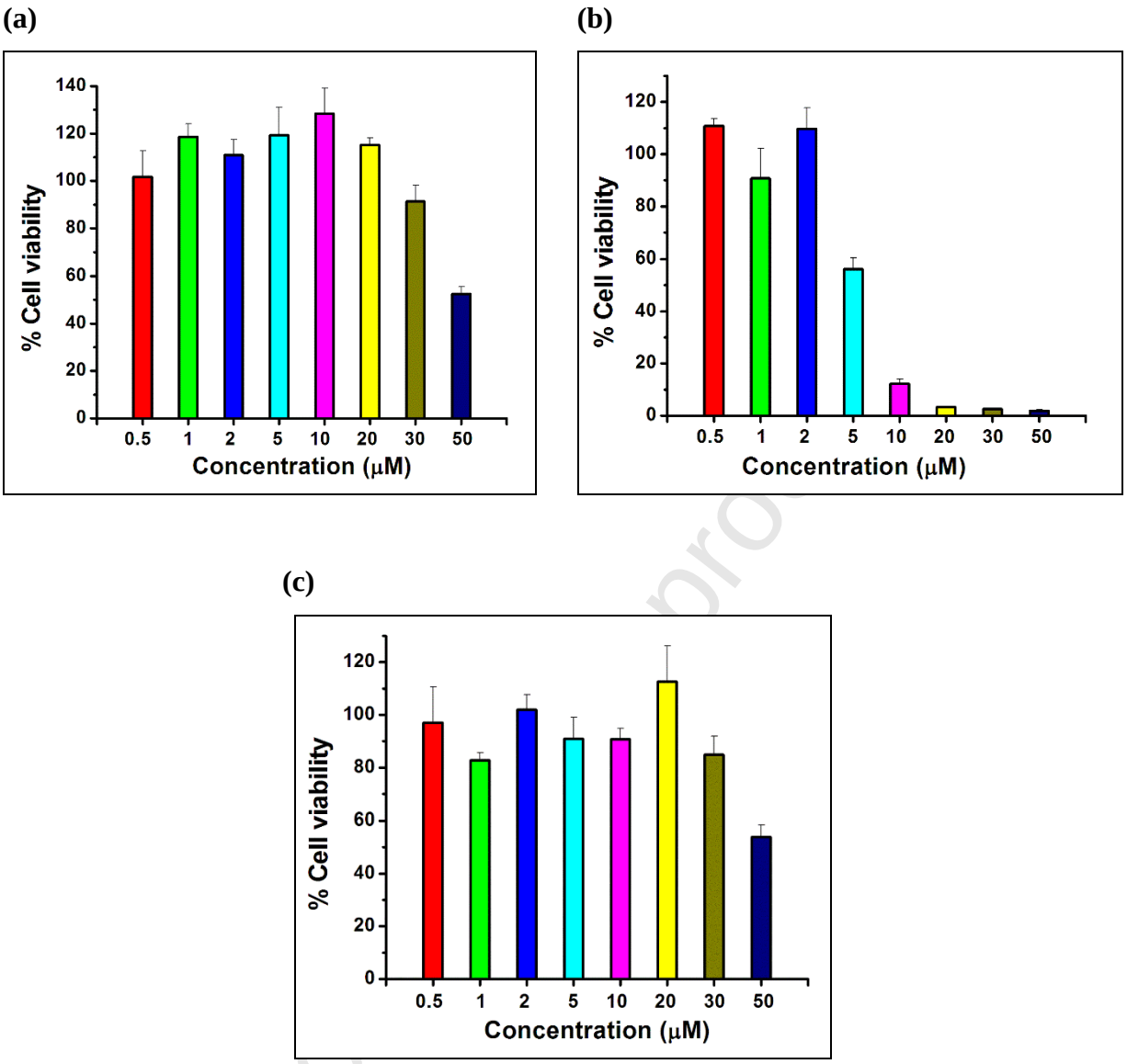

Figure 13. % cell viability of A549 cells after exposure to **(a) 1**, **(b) 2**, and **(c) 3**, for 48 h.

4. Conclusions

In this study, three mononuclear copper(II) complexes (**1**, **2** and **3**) derived from a novel benzothiazole based ligand (*N*-(benzo[d]thiazol-2-ylmethyl)-N-methyl-2-(pyridin-2-yl)ethan-1-amine) have been synthesized and structurally characterized. Complexes **1** and **3** are water soluble but complex **2** has very limited aqueous solubility. DNA and BSA binding with water-soluble complexes **1** and **3** have been evaluated and the binding constants for both the complexes are in a similar range. DNA cleavage study, antioxidant studies and cellular studies are performed for **2** were carried out using organic solvents as vehicle. All the complexes show

efficient DNA nuclease activity of the double-stranded pET-28b plasmid. In addition to the oxidative DNA cleavage, complex **1** and **3** also show prominent hydrolytic DNA cleavage. In spite of weak binding to DNA, the complexes show potent concentration-dependent nuclease activity suggesting a different mechanism of interaction of the complexes with DNA. The major difference in the activity of the complexes due to the difference in the co-ligand was observed in cytotoxicity against lung cancer A549 cell lines. Only complex **2** having rhodanide (-NCS) as co-ligand, showed good anti-proliferative activity with an IC_{50} value in low micromolar range. The other two complexes have very low potency against the cell line tested. Taken together, it is concluded that more than one mechanism is in action for the observed cell toxicity behaviors' of these complexes. In addition, complex **2** exhibits potential antioxidant properties that are considered relevant for the development of therapeutic agents. The current study lays the groundwork for the development of benzothiazole and -NCS based copper(II) complexes for therapeutic purposes.

Conflicts of interest

There are no competing financial interests to declare.

Dedication

This manuscript is dedicated to Prof. Samaresh Bhattacharya on his 60th Birthday.

Acknowledgements

AKS acknowledges the support from UGC-BSR Research Start-up-grant (ref. no. F.30.414/2018(BSR)), DST-SERB EMR grant (ref. no. EMR/2016/001452) and DST-INSPIRE research grant (IFA-13, CH-97). SJ is thankful to DST-INSPIRE for Senior Research Fellowship (IF150116), while KB acknowledges SERB for NPDF (PDF/2017/000929). SB thanks the Central University of Rajasthan for providing the university fellowship and CCM is thankful for the DST-RFBR grant (INT/RUS/RFBR/P-256). VKS is grateful to UGC for JRF, and ST acknowledges DST-SERB grants (YSS/2015/000138, and EEQ/2016/000569). The authors acknowledge the instrumental facilities at the Department of Chemistry, Central University of Rajasthan supported by DST-FIST (ref. no. SR/FST/CSI-257/2014(C)). The authors are also thankful to the University of Burdwan, West Bengal for single-crystal X-ray crystallographic data collection.

References

[1] World Health Organization, Cancer (2018). https://www.who.int/news-room/fact-sheets/detail/cancer.

[2] B. Rosenberg, L. Vancamp, T. Krigas, Inhibition of Cell Division in Escherichia Coli by Electrolysis Products from a Platinum Electrode, Nature. 205 (1965) 698-699. http://doi.org/10.1038/205698a0

[3] X. Wang, Z. Guo, Towards the rational design of platinum (II) and gold (III) complexes as antitumour agents, Dalton Trans. (2008) 1521-1532. http://doi.org/10.1039/B715903J

[4] I. Kostova, Gold coordination complexes as anticancer agents, Anti-Cancer Agents in Med. Chem. 6 (2006) 19-32. http://doi.org/10.2174/187152006774755500

[5] K. Irena, Ruthenium Complexes as Anticancer Agents, Curr. Med. Chem. 13 (2006) 1085-1107. http://dx.doi.org/10.2174/092986706776360941

[6] M.J. Hannon, Metal-based anticancer drugs: From a past anchored in platinum chemistry to a post-genomic future of diverse chemistry and biology, Pure Appl. Chem. 79 (2007) 2243-2261. http://doi.org/10.1351/pac200779122243

[7] D. Gaynor, D.M. Griffith, The prevalence of metal-based drugs as therapeutic or diagnostic agents: beyond platinum, Dalton Trans. 41 (2012) 13239-13257. http://dx.doi.org/10.1039/C2DT31601C

[8] D. Wernitznig, K. Kiakos, G. Del Favero, N. Harrer, H. Machat, A. Osswald, M.A. Jakupec, A. Wernitznig, W. Sommergruber, B.K. Keppler, First-in-class ruthenium anticancer drug (KP1339/IT-139) induces an immunogenic cell death signature in colorectal spheroids in vitro, Metallomics (2019). http://dx.doi.org/10.1039/C9MT00051H

[9] S. Zorzet, A. Sorc, C. Casarsa, M. Cocchietto, G. Sava, Pharmacological effects of the ruthenium complex NAMI-A given orally to CBA mice with MCa mammary carcinoma, Met. based drugs. 8 (2001) 1-7. http://doi.org/10.1155/mbd.2001.1

[10] P.-S. Kuhn, V. Pichler, A. Roller, M. Hejl, M. Jakupec, W. Kandioller, B. Keppler, Improved reaction conditions for the synthesis of new NKP-1339 derivatives and preliminary investigations on their anticancer potential, Dalton Trans. 44 (2015) 659-668. http://doi.org/10.1039/c4dt01645a

[11] C.K. Osborne, Tamoxifen in the treatment of breast cancer, N. Engl. J. Med. 339 (1998) 1609-1618. http://doi.org/10.1056/nejm199811263392207

[12] M. Wehbe, A.W.Y. Leung, M.J. Abrams, C. Orvig, M.B. Bally, A Perspective – can copper complexes be developed as a novel class of therapeutics?, Dalton Trans. 46 (2017) 10758-10773. http://dx.doi.org/10.1039/C7DT01955F

[13] S. Monro, K.L. Colón, H. Yin, J. Roque, P. Konda, S. Gujar, R.P. Thummel, L. Lilge, C.G. Cameron, S.A. McFarland, Transition Metal Complexes and Photodynamic Therapy from a Tumor-Centered Approach: Challenges, Opportunities, and Highlights from the Development of TLD1433, Chem Rev. 119 (2019) 797-828. http://doi.org/10.1021/acs.chemrev.8b00211

[14] R.G. Kenny, C.J. Marmion, Toward Multi-Targeted Platinum and Ruthenium Drugs—A New Paradigm in Cancer Drug Treatment Regimens?, Chem Rev. 119 (2019) 1058-1137. http://doi.org/10.1021/acs.chemrev.8b00271

[15] B. Englinger, C. Pirker, P. Heffeter, A. Terenzi, C.R. Kowol, B.K. Keppler, W. Berger, Metal Drugs and the Anticancer Immune Response, Chem Rev. 119 (2019) 1519-1624. http://doi.org/10.1021/acs.chemrev.8b00396

[16] J.R. Lou, X.-X. Zhang, J. Zheng, W.-Q. Ding, Transient Metals Enhance Cytotoxicity of Curcumin: Potential Involvement of the NF-κB and mTOR Signaling Pathways, Anticancer Res. 30 (2010) 3249-3255

[17] A. Mookerjee, J.M. Basu, S. Majumder, S. Chatterjee, G.S. Panda, P. Dutta, S. Pal, P. Mukherjee, T. Efferth, S. Roy, S.K. Choudhuri, A novel copper complex induces ROS generation in doxorubicin resistant Ehrlich ascitis carcinoma cells and increases activity of antioxidant enzymes in vital organs in vivo, BMC Cancer. 6 (2006) 267-267. http://doi.org/10.1186/1471-2407-6-267

[18] Z. Zhang, H. Wang, M. Yan, H. Wang, C. Zhang, Novel copper complexes as potential proteasome inhibitors for cancer treatment, Mol. Med. Rep. 15 (2017) 3-11. http://doi.org/10.3892/mmr.2016.6022

[19] I. Iakovidis, I. Delimaris, S.M. Piperakis, Copper and its complexes in medicine: a biochemical approach, Mol. Biol. Int. 2011 (2011) 594529. http://doi.org/10.4061/2011/594529

[20] L. Polloni, A.C.d. Seni Silva, S.C. Teixeira, F.V.P.d.V. Azevedo, M.A.P. Zóia, M.S. da Silva, P.M.A.P. Lima, L.I.V. Correia, J. do Couto Almeida, C.V. da Silva, V.d.M. Rodrigues Ávila, L.R.F. Goulart, S. Morelli, W. Guerra, R.J.d. Oliveira Júnior, Action of copper(II)

complex with β-diketone and 1,10-phenanthroline (CBP-01) on sarcoma cells and biological effects under cell death, Biomedicine & Pharmacotherapy. 112 (2019) 108586. http://doi.org/10.1016/j.biopha.2019.01.047

[21] X. Qiao, Z.-Y. Ma, J. Shao, W.-G. Bao, J.-Y. Xu, Z.-Y. Qiang, J.-S. Lou, Biological evaluation of a cytotoxic 2-substituted benzimidazole copper (II) complex: DNA damage, antiproliferation and apoptotic induction activity in human cervical cancer cells, Biometals. 27 (2014) 155-172. http://doi.org/10.1007/s10534-013-9696-1

[22] F. Tisato, C. Marzano, M. Porchia, M. Pellei, C. Santini, Copper in diseases and treatments, and copper-based anticancer strategies, Med. Res. Rev. 30 (2010) 708-749. http://doi.org/10.1002/med.20174

[23] C. Santini, M. Pellei, V. Gandin, M. Porchia, F. Tisato, C. Marzano, Advances in Copper Complexes as Anticancer Agents, Chem Rev. 114 (2014) 815-862. http://doi.org/10.1021/cr400135x

[24] I. Gracia-Mora, L. Ruiz-Ramírez, C. Gómez-Ruiz, M. Tinoco-Méndez, A. Márquez-Quiñones, L.R.-D. Lira, l. Marín-Hernández, L. Macías-Rosales, M.E. Bravo-Gómez, Knigth's Move in the Periodic Table, From Copper to Platinum, Novel Antitumor Mixed Chelate Copper Compounds, Casiopeinas, Evaluated by an in Vitro Human and Murine Cancer Cell Line Panel, Met. Based Drugs. 8 (2001) 19-28. http://doi.org/10.1155/mbd.2001.19

[25] T. McGivern, S. Afsharpour, C. Marmion, Copper complexes as artificial DNA metallonucleases: from Sigman's reagent to next generation anti-cancer agent?, Inorg. Chim. Acta. 472 (2018) 12-39. http://doi.org/10.1016/j.ica.2017.08.043

[26] L. Ruiz-Azuara, G. Bastian, M.E. Bravo-Gómez, R.C. Cañas, M. Flores-Alamo, I. Fuentes, C. Mejia, J.C. García-Ramos, A. Serrano, Abstract CT408: Phase I study of one mixed chelates copper (II) compound, Casiopeína CasIIIia with antitumor activity and its mechanism of action, Cancer Res. 74 (2014). 10.1158/1538-7445.AM2014-CT408

[27] R. Tabti, N. Tounsi, C. Gaiddon, E. Bentouhami, L. Désaubry, Progress in copper complexes as anticancer agents, Med. Chem. 7 (2017) 875-879. http://doi.org.10.4172/2161-0444.1000445

[28] C. Marzano, M. Pellei, F. Tisato, C. Santini, Copper complexes as anticancer agents, Anticancer Agents Med. Chem. 9 (2009) 185-211. http://doi.org/10.2174/187152009787313837

[29] C.S. Devi, B. Thulasiram, R.R. Aerva, P. Nagababu, Recent Advances in Copper Intercalators as Anticancer Agents, J. Fluoresc. 28 (2018) 1195-1205. http://doi.org/10.1007/s10895-018-2283-7

[30] C. Wende, C. Lüdtke, N. Kulak, Copper Complexes of N-Donor Ligands as Artificial Nucleases, Eur. J. Inorg. Chem. 2014 (2014) 2597-2612. http://doi.org/10.1002/ejic.201400032

[31] S. Tardito, L. Marchio, Copper compounds in anticancer strategies, Curr. Med. Chem. 16 (2009) 1325-1348. http://doi.org/10.2174/092986709787846532

[32] P.C. Sharma, A. Sinhmar, A. Sharma, H. Rajak, D.P. Pathak, Medicinal significance of benzothiazole scaffold: an insight view, J. Enzyme Inhib. Med. Chem. 28 (2013) 240-266. http://doi.org/10.3109/14756366.2012.720572

[33] A. Kamal, M.A.H. Syed, S.M. Mohammed, Therapeutic potential of benzothiazoles: a patent review (2010–2014), Expert Opin. Ther. Pat. 25 (2015) 335-349. http://doi.org/10.1517/13543776.2014.999764

[34] X. Fu, G. Weng, D. Liu, S. Le XY, Synthesis, characterization, DNA binding and cleavage, HSA interaction and cytotoxicity of a new copper (II) complex derived from 2-(2-pyridyl) benzothiazole and glycylglycine, J. Photochem. Photobiol. A. 276 (2014) 83-95. http://doi.org/10.1016/j.jphotochem.2013.12.002

[35] P.U. Maheswari, M.v.d. Ster, S. Smulders, S. Barends, G.P.v. Wezel, C. Massera, S. Roy, H.d. Dulk, P. Gamez, J. Reedijk, Structure, Cytotoxicity, and DNA-Cleavage Properties of the Complex [Cu(II)(pbt)Br_2], Inorg. Chem. 47 (2008) 3719-3727. http://doi.org/10.1021/ic702306f

[36] Y. Lu, Y. Chen, Z. Ou, S. Chen, C. Zhuang, X. Le, Synthesis, Antibacterial Activities and Nuclease Properties of Ternary Copper (II) Complex Containing 2-(2′-Pyridyl) benzothiazole and Glycinate, Chin. J. Chem. 30 (2012) 303-310. http://doi.org/10.1002/cjoc.201100169

[37] S.-Z. Hu, D. Shi, T. Huang, J. Wan, Z. Huang, J. Yang, C. Xu, Crystal structures and antitumour activity of 2-(2′-pyridyl)benzothiazole and its organotin complex, Inorg. Chim. Acta. 173 (1990) 1-4. http://doi.org/10.1016/S0020-1693(00)91046-6

[38] A. Lewis, M. McDonald, S. Scharbach, S. Hamaway, M. Plooster, K. Peters, K.M. Fox, L. Cassimeris, J.M. Tanski, L.A. Tyler, The chemical biology of Cu (II) complexes with imidazole or thiazole containing ligands: Synthesis, crystal structures and comparative biological activity, J. Inorg. Biochem. 157 (2016) 52-61. http://doi.org/10.1016/j.jinorgbio.2016.01.014

[39] R.A. Steiner, D. Foreman, H.X. Lin, B.K. Carney, K.M. Fox, L. Cassimeris, J.M. Tanski, L.A. Tyler, Synthesis, characterization, crystal structures and biological activity of set of Cu (II) benzothiazole complexes: Artificial nucleases with cytotoxic activities, J. Inorg. Biochem. 137 (2014) 1-11. http://doi.org/10.1016/j.jinorgbio.2014.04.002

[40] X. Yue, Y. Chen, G. Yang, S. Yue, Z. Su, Synthesis, crystal structures and DNA-binding properties of Cd (II), Cu (II) and Ni (II) complexes with 2-(2-pyridyl) benzothiazole, Synth. Met. 200 (2015) 1-6. http://doi.org/10.1016/j.synthmet.2014.12.022

[41] M.E. Reichmann, S.A. Rice, C.A. Thomas, P. Doty, A Further Examination of the Molecular Weight and Size of Desoxypentose Nucleic Acid, J. Am. Chem. Soc. 76 (1954) 3047-3053. http://doi.org/10.1021/ja01640a067

[42] K. Peprah, X.Y. Zhu, S.V. Eyunni, J.R. Etukala, V. Setola, B.L. Roth, S.Y. Ablordeppey, Structure–activity relationship studies of SYA 013, a homopiperazine analog of haloperidol, Bioorg. Med. Chem. 20 (2012) 1671-1678. http://doi.org/10.1016/j.bmc.2012.01.022

[43] I. Ali, W.A. Wani, K. Saleem, Empirical formulae to molecular structures of metal complexes by molar conductance, Synthesis and Reactivity in Inorganic, Metal-Organic, and Nano-Metal Chemistry. 43 (2013) 1162-1170. http://doi.org/10.1080/15533174.2012.756898

[44] G.M. Sheldrick, SHELXT - integrated space-group and crystal-structure determination, Acta Cryst. A 71 (2015) 3-8. http://doi.org/10.1107/S2053273314026370

[45] G. Sheldrick, Crystal structure refinement with SHELXL, Acta Cryst. C. 71 (2015) 3-8. http://doi.org/10.1107/S2053229614024218

[46] A. Spek, Single-crystal structure validation with the program PLATON, J. Appl. Cryst. 36 (2003) 7-13. http://doi.org/10.1107/S0021889802022112

[47] O.V. Dolomanov, L.J. Bourhis, R.J. Gildea, J.A.K. Howard, H. Puschmann, OLEX2: a complete structure solution, refinement and analysis program, J. Appl. Cryst. 42 (2009) 339-341. http://dx.doi.org/10.1107/S0021889808042726

[48] K. Chowdhury, A. Sharma, S. Kumar, G.K. Gunjan, A. Nag, C.C. Mandal, Colocynth extracts prevent epithelial to mesenchymal transition and stemness of breast cancer cells, Front. Pharmacol. 8 (2017) 593. http://doi.org/10.3389/fphar.2017.00593

[49] A. Sharma, S. Bandyopadhayaya, K. Chowdhury, T. Sharma, R. Maheshwari, A. Das, G. Chakrabarti, V. Kumar, C.C. Mandal, Metformin exhibited anticancer activity by lowering

cellular cholesterol content in breast cancer cells, PLOS ONE. 14 (2019) e0209435. http://doi.org/10.1371/journal.pone.0209435

[50] V. Sathyanarayanmoorthi, R. Karunathan, V. Kannappan, Molecular modeling and spectroscopic studies of benzothiazole, J. Chem (2013). http://doi.org/10.1155/2013/258519

[51] C. Baer, J. Pike, Infrared spectroscopic analysis of linkage isomerism in metal− thiocyanate complexes, J. Chem. Educ. 87 (2010) 724-726. http://doi.org/10.1021/ed100284z

[52] A.B.P. Lever Journal (1984) Pages.

[53] A.B.P. Lever, Electronic Spectra of Some Transition Metal Complexes, J. Chem. Educ. 45 (1968) 711-712. http://doi.org/10.1021/ed045p711

[54] E. Garribba, G. Micera, The determination of the geometry of Cu(II) complexes - An EPR spectroscopy experiment, J. Chem. Educ. 83 (2006) 1229-1232. http://doi.org/10.1021/ed083p1229

[55] J. Peisach, W.E. Blumberg, Structural implications derived from the analysis of electron paramagnetic resonance spectra of natural and artificial copper proteins, Arch. Biochem. Biophy. 165 (1974) 691-708. http://doi.org/10.1016/0003-9861(74)90298-7

[56] A.W. Addison, T.N. Rao, J. Reedijk, J. van Rijn, G.C. Verschoor, Synthesis, structure, and spectroscopic properties of copper(II) compounds containing nitrogen-sulphur donor ligands; the crystal and molecular structure of aqua[1,7-bis(N-methylbenzimidazol-2[prime or minute]-yl)-2,6-dithiaheptane]copper(II) perchlorate, J. Chem. Soc., Dalton Trans. (1984) 1349-1356. http://dx.doi.org/10.1039/DT9840001349

[57] K. Marjani, M. Mousavi, D.L. Hughes, Synthesis and crystal structure determination of copper (II) and iron (III) complexes of 2-(2-pyridyl) benzothiazole, Transit. Met. Chem. 34 (2009) 85. http://doi.org.10.1007/s11243-008-9161-0

[58] Z.W. Schroeder, L. Hiscock, L.N. Dawe, Copper (II)-and gold (III)-mediated cyclization of a thiourea to a substituted 2-aminobenzothiazole, Acta Cryst. C. 73 (2017) 905-910. http://doi.org/10.1107/S205322961701381X

[59] H.-K. Liu, P.J. Sadler, Metal complexes as DNA intercalators, Acc. Chem. Res. 44 (2011) 349-359. http://doi.org/10.1021/ar100140e

[60] S. Jain, K. Bhar, S. Kumar, S. Bandyopadhyaya, S. Tapryal, C.C. Mandal, A.K. Sharma, Homo- and heteroleptic trimethoxy terpyridine–Cu(ii) complexes: synthesis, characterization,

DNA/BSA binding, DNA cleavage and cytotoxicity studies, Dalton Trans. 49 (2020) 4100-4113. http://dx.doi.org/10.1039/D0DT00209G

[61] K. Sangeetha Gowda, B.B. Mathew, C. Sudhamani, H. Naik, Mechanism of DNA binding and cleavage, J. Biomed. Biotechnol. 2 (2014) 1-9. http://www.doi.org/10.12691/bb-2-1-1

[62] C.J. Burrows, J.G. Muller, Oxidative nucleobase modifications leading to strand scission, Chem. Rev. 98 (1998) 1109-1152. http://doi.org/10.1021/cr960421s

[63] W.K. Pogozelski, T.D. Tullius, Oxidative strand scission of nucleic acids: routes initiated by hydrogen abstraction from the sugar moiety, Chem. Rev. 98 (1998) 1089-1108. http://doi.org/10.1021/cr960437i

[64] D.S. Sigman, A. Mazumder, D.M. Perrin, Chemical nucleases, Chem. Rev. 93 (1993) 2295-2316. http://doi.org/10.1021/cr00022a011

[65] G. Pratviel, J. Bernadou, B. Meunier, Carbon—hydrogen bonds of DNA sugar units as targets for chemical nucleases and drugs, Angew. Chem. Int. Ed. 34 (1995) 746-769. http://doi.org/10.1002/anie.199507461

[66] Q. Jiang, N. Xiao, P. Shi, Y. Zhu, Z. Guo, Design of artificial metallonucleases with oxidative mechanism, Coord. Chem. Rev. 251 (2007) 1951-1972. http://doi.org/10.1016/j.ccr.2007.02.013

[67] N. Kochetkov, E. Budovskii, Organic Chemistry of Nucleic Acids, Springer, 1972, pp. 381-423.

[68] R. Stoewe, W.A. Prütz, Copper-catalyzed DNA damage by ascorbate and hydrogen peroxide: kinetics and yield, Free Radic. Biol. Med. 3 (1987) 97-105. http://doi.org/10.1016/S0891-5849(87)80003-5

[69] F. Wang, P. Jiao, M. Qi, M. Frezza, Q. Dou, B. Yan, Turning tumor-promoting copper into an anti-cancer weapon via high-throughput chemistry, Curr. Med. Chem. 17 (2010) 2685-2698. http://doi.org/10.2174/092986710791859315

[70] U.S. Srinivas, B.W. Tan, B.A. Vellayappan, A.D. Jeyasekharan, ROS and the DNA damage response in cancer, Redox Biology. 25 (2019) 101084. http://doi.org/10.1016/j.redox.2018.101084

[71] T. Topală, A. Bodoki, L. Oprean, R. Oprean, Bovine Serum Albumin Interactions with Metal Complexes, Clujul Med. 87 (2014) 215-219. http://doi.org/10.15386/cjmed-357

[72] N. Singh, D. Pagariya, S. Jain, S. Naik, N. Kishore, Interaction of copper (II) complexes by bovine serum albumin: Spectroscopic and calorimetric insights, J. Biomol. Struct. Dyn. 36 (2018) 2449-2462. http://doi.org/10.1080/07391102.2017.1355848

[73] M.R. Eftink, C.A. Ghiron, Fluorescence quenching studies with proteins, Anal. Biochem. 114 (1981) 199-227. http://doi.org/10.1016/0003-2697(81)90474-7

[74] J. Miller, Photoluminescence and chemiluminescence methods of drug analysis, J. Pharm. Biomed. Anal. 1 (1983) 525-535. http://doi.org/10.1016/0731-7085(83)80066-1

[75] N. Sudha, Y. Sameena, S. Chandrasekaran, I.V. Enoch, D. Premnath, Alteration of the binding strength of dronedarone with bovine serum albumin by β-cyclodextrin: a spectroscopic study, Spectrosc. Lett. 48 (2015) 112-119. http://doi.org/10.1080/00387010.2013.858052

[76] X. Zhang, Y. Lin, L. Liu, C. Lin, Study on the synthesis of sulfonamide derivatives and their interaction with bovine serum albumin, J. Lumin. 30 (2015) 269-279. http://doi.org/10.1002/bio.2725

[77] B. Halliwell, Establishing the significance and optimal intake of dietary antioxidants: the biomarker concept, Nutr. Rev. 57 (1999) 104-113. http://doi.org/10.1111/j.1753-4887.1999.tb06933.x

[78] U. Bandyopadhyay, D. Das, R.K. Banerjee, Reactive oxygen species: oxidative damage and pathogenesis, Curr. Sci. (1999) 658-666. http://www.jstor.org/stable/24102839

[79] B. Halliwell, R. Aeschbach, J. Löliger, O. Aruoma, The characterization of antioxidants, Food Chem. Toxicol. 33 (1995) 601-617. http://doi.org/10.1016/0278-6915(95)00024-v

[80] S. Cuzzocrea, D.P. Riley, A.P. Caputi, D. Salvemini, Antioxidant therapy: a new pharmacological approach in shock, inflammation, and ischemia/reperfusion injury, Pharmacol. Rev. 53 (2001) 135-159

[81] X. Shi, H. Fang, Y. Guo, H. Yuan, Z. Guo, X. Wang, Anticancer copper complex with nucleus, mitochondrion and cyclooxygenase-2 as multiple targets, J. Inorg. Biochem. 190 (2019) 38-44. http://doi.org/10.1016/j.jinorgbio.2018.10.003

[82] A.P. Vieira, C.A. Wegermann, A.M.D.C. Ferreira, Comparative studies of Schiff base-copper (II) and zinc (II) complexes regarding their DNA binding ability and cytotoxicity against sarcoma cells, New J. Chem. 42 (2018) 13169-13179. http://doi.org/10.1039/C7NJ04799A

[83] D. Mahendiran, R.S. Kumar, V. Viswanathan, D. Velmurugan, A.K. Rahiman, In vitro and in vivo anti-proliferative evaluation of bis (4′-(4-tolyl)-2, 2′: 6′, 2 ″-terpyridine) copper (II)

complex against Ehrlich ascites carcinoma tumors, J. Biol. Inorg. Chem. 22 (2017) 1109-1122. http://doi.org/10.1007/s00775-017-1488-6

[84] V.T. Yilmaz, C. Icsel, F. Suyunova, M. Aygun, N. Aztopal, E. Ulukaya, Ni (II)/Cu (II)/Zn (II) 5, 5-diethylbarbiturate complexes with 1, 10-phenanthroline and 2, 2′-dipyridylamine: Synthesis, Structures, DNA/BSA binding, Nuclease activity, Molecular docking, Cellular uptake, Cytotoxicity and the Mode of Cell Death, Dalton Trans. 45 (2016) 10466-10479. http://doi.org/10.1039/c6dt01726f

[85] Z.-Y. Ma, X. Qiao, C.-Z. Xie, J. Shao, J.-Y. Xu, Z.-Y. Qiang, J.-S. Lou, Activities of a novel Schiff Base copper (II) complex on growth inhibition and apoptosis induction toward MCF-7 human breast cancer cells via mitochondrial pathway, J. Inorg. Biochem. 117 (2012) 1-9. http://doi.org/10.1016/j.jinorgbio.2012.08.007

Graphical Abstract

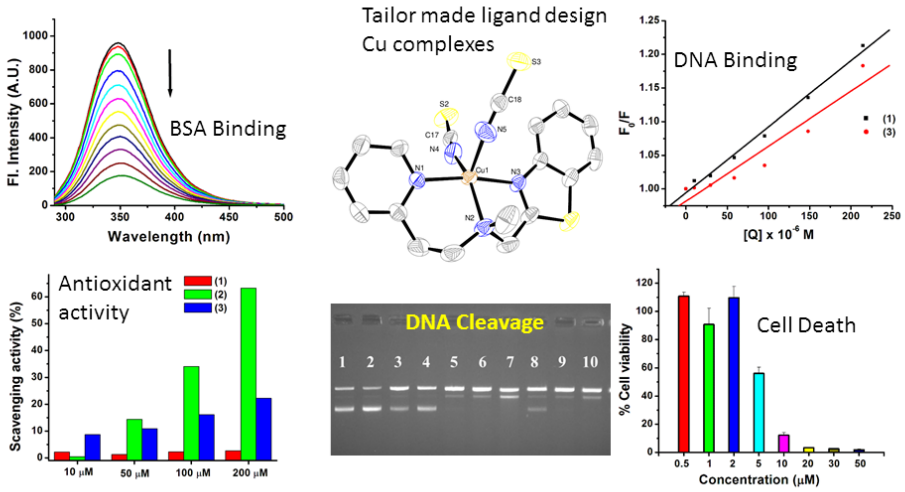

A novel benzothiazole derived tridentate ligand is utilized for the synthesis of copper(II) complexes with a motive to develop new Cu complexes for therapeutic purposes. Studies on DNA binding, protein binding, nuclease activity, antioxidant activity, and cytotoxicity on lung cancer (A549) cell line are described.

Highlights

1. Development of benzothiazole based Cu(II) complexes for therapeutic purposes
2. Detailed characterization by various methods including single-crystal X-ray diffraction
3. DNA binding and nuclease activity showing hydrolytic and oxidative cleavage of DNA
4. BSA binding and antioxidant properties have been evaluated
5. Cytotoxicity study on lung cancer (A549) cell line showing antiproliferative activity